Chapter 4
Lignin Degrading Fungal Enzymes

Ayyappa Kumar Sista Kameshwar and Wensheng Qin

4.1 Introduction

Lignin is the most complex and abundant naturally occurring biopolymer present in plant cell walls. It forms a tight matrix around the carbohydrates, and it is closely associated with cellulose, hemicellulose and pectin, forming an intricate structure. Lignin provides several advantages to the plant cell wall such as mechanical strength supporting large plant structures, protection against microbial infections as it is hard to degrade, impermeability and stability against chemical and mechanical attacks [1]. Lignin is an aromatic polymer made up of three basic units: p-coumaryl alcohol (4-hydroxycinnamyl alcohol), coniferyl alcohol and sinapyl alcohol which are collectively called monolignols that are derived from phenylalanine (aromatic amino acid) [2]. Monolignols produce three phenylproponoid units, p-hydroxyphenyl (H), syringyl alcohol (S), guaiacyl (G) later these units are collectively joined to form the lignin polymer [3]. The percentage of the different phenylproponoids present in lignin varies based on the type of cell, taxa, wood, environment and developmental conditions. Lignin present in dicotyledonous angiosperms contains mainly G and S, with traces of H units. Gymnosperms, contain high G and low H and, grasses (Monocots) contain high H units with, comparable G and S units [3]. Lignin contains several interionic bonds such as alkyl-alkyl, aryl-alkyl and aryl-aryl, lignin also associates with plant cell wall polysaccharides which makes the breakdown and separation of lignin very difficult [4]. Separation of lignin from lignocellulosic materials is not possible without partial disruption of the lignocellulosic network. During plant cell wall polymerization several intermediates are produced and, these intermediates react with oligolignols, carboxyl and hydroxyl groups of glucuronic acids in hemicellulose units resulting in ethers and esters [5–7]. Research groups

A.K.S. Kameshwar • W. Qin (✉)
Department of Biology, Lakehead University,
955 Oliver Road, P7B 5E1 Thunder Bay, ON, Canada
e-mail: wqin@lakeheadu.ca

Z. Fang, R.L. Smith, Jr. (eds.), *Production of Biofuels and Chemicals from Lignin*, Biofuels and Biorefineries 6, DOI 10.1007/978-981-10-1965-4_4

have tried to efficiently separate lignin from lignocellulosic biomass (cellulose, hemicellulose) for production of cellulosic ethanol (biofuels). Biofuel and paper pulp industries make use of cellulose for the production of paper and cellulosic ethanol, leaving behind hemicellulose and lignin as industrial effluents. The depolymerization of the polyphenolic chemical structure of lignin offers many opportunities for producing conventional phenolic compounds [8].

Several studies have showed that lignin is resistant to the microbial attack however a few groups of microorganisms belonging to bacteria and fungi are able to efficiently degrade lignin [9]. It has been reported that anaerobic processes fail to attack aromatic rings while aerobic processes tend to degrade lignin [7, 9]. Fungi are the most studied organisms for lignin degradation. Basidiomycota phylum consists of a wide range of wood degrading fungi, thus it is the largest wood degrading fungal group [10, 11]. Wood degrading fungi belonging to Basidiomycota phylum can be further divided into white, brown and soft rotting fungi based on their wood decaying patterns. In the Basidiomycota phylum, most of the wood degrading fungi belong to the Agaricales and Aphyllophorales orders [12]. White rot fungi are considered to be the most efficient lignin degraders, but their degradation rates for lignin and cellulose in wood tissue vary considerably [13]. Some white rot fungi are able to selectively degrade lignin without degrading much cellulose while other white rot fungi are able to attack both lignin and carbohydrates. However, fungi which are able to selectively degrade lignin are of higher significance due to their commercial applications (e.g. paper and pulp industries) [10, 13]. White rot fungi secrete a wide range of wood degrading enzymes that are involved in the breakdown of carbohydrate components (cellulose and hemicellulose) and lignin. White rot fungi secrete different lignin degrading enzymes such as lignin peroxidase, manganese dependent peroxidase, laccase, horse radish peroxidase, and dioxygenases such as protocatechuate 3,4 dioxygenase, 1,2,4-trihydroxybenzene 1,2-dioxygenase, catechol 1,2-dioxygenase, superoxide dismutase, glyoxal oxidase, glucose 1-oxidase, aryl alcohol oxidase, veratryl alcohol oxidase, pyranose oxidase and, quinone oxidoreductase [13, 14]. When compared to white rot fungi, brown rot fungi are more efficient in degrading cellulose and hemicellulose than lignin, however these fungi potentially modify lignin [10]. Wood affected by brown rot fungi generally appears shrunken and dark in color with brick and cubical shaped fragments, these fragments can be easily broken down further to a brown color powder (modified lignin). Wood decaying fungi belonging to the phyla Ascomycota and Deuteromycota are mostly soft rot fungi, these fungi usually decay wood, causing a light brown color. Based on the patterns they form on the wood these fungi can be further classified into type I (form biconical or cylindrical cavities in secondary walls) and type II (this type of fungi cause erosion). When compared to white rot fungi, type II soft rot fungi do not attack the middle lamella (Table 4.1) [10]. Some basidiomycete fungi form unique symbiotic associations with wood degrading termites belonging to Termitomyces, Bacteroidetes and Firmicutes classes. Some bacteria and flagellated protists also resides in the termite hind gut [7]. Both lower and higher termites maintain a remarkable microbial diversity in their guts and, some

Table 4.1 Illustrates potential wood degrading fungal phylum and their properties

Type of wood degradation	Phyla and order	Wood degradation property	Decaying wood	Fungal strain
White Rot	Basidiomycota:	Causes cell wall erosion in cell lumina by occupying large spaces with its mycelium.	Moist, spongy appearance white or yellow	*Phanerochaete chrysosporium, Ceriporiopsus subvermispora*,
	Agaricales Aphyllophorales	Efficiently degrade lignin.		
Brown Rot	Basidiomycota:	Penetrates through cell wall pores, by effecting the S2 layer of cell wall in lumen.	Dry, shrunken, cracked, in brown colored fragments	*Gleophylum trabeum, Postia placenta*,
	Agaricales Aphyllophorales	Efficiently degrades cellulose and hemicellulose.		*Serpula lacrymans*,
Soft Rot	Ascomycota:	Type I fungi forms cylindrical, biconical cavities in secondary cell walls.	Decayed wood is brown in color with soft look which further cracks and becomes dry.	*Fusarium solani, Penicillium chrysogenum, Daldinia concentrica*
	Deuteromycota	Type II fungi are erosive wood degraders.		

bacteria were found to colonize in hindgut, fore and midgut. Termites depend on their gut microbiota for their nutrition, as most of their nutrition is derived from the downstream products of microbial metabolism [7]. The underlying mechanisms behind the utilization and degradation of lignocellulose biomass by termites was only revealed recently. Genome sequencing and metagenome sequencing (termite gut microbiome) studies conducted on different lignocellulose degrading fungi have revealed several interesting facts about lignin degradation [15].

4.2 Carbohydrate Active Enzyme Database (CAZy)

CAZy is a sequence based classification of the enzymes which are involved in the formation, modification and breakdown of poly and oligosaccharides [16]. There are three major defining features underlying CAZyme classification, (a) Classification is based on significant similarity of amino acid sequences with a

minimum of one biochemically characterized founding member (b) CAZymes generally are modular proteins with a catalytic module containing different discrete units, thus it is classified module by module [17]. Third important feature CAZyme classification is based on systematical protein sequences upon daily GenBank releases which avoids analyzing unfinished protein sequences with changing accession numbers. The CAZy database is currently divided into two main classes as Carbohydrate active enzymes and Carbohydrate binding modules (CBMs). Carbohydrate active enzymes are further divided into five classes they are (a) Glycoside hydrolases (GH) (b) Glycosyl Transferases (GT) (c) Polysaccharide Lyases (PL) (d) Auxiliary Activity enzymes (AA) (e) Carbohydrate Esterases [16]. Carbohydrate binding modules (CBMs) earlier known as Cellulose binding modules, recent discovery of several new binding modules which bind to carbohydrates other than cellulose was the main reason behind the name change to carbohydrate binding modules. The occurrence of lignin in close associations with other polysaccharides (cellulose and hemicellulose) in plant cell walls led to, lignin degrading enzymes and lytic polysaccharide monoxygenases (LPMO) to be classified into "Auxiliary activity enzymes" among the large class of enzymes involved in the modification and breakdown of lignocellulose. Auxiliary activity enzymes are currently classified into three subfamilies of polysaccharide monoxygenases and eight classes of lignolytic enzymes, a total of 1045 enzymes were classified into 13 subfamilies and 304 non classified enzymes [16]. CAZy database can be used to analyze the genomes (Carbohydrate active enzymes encoded in the genome of an organism CAZome), and also to study the molecular details of substrate recognition. CAZome can provide significant insights about the nature and amount of metabolism of complex carbohydrates by a species. At present the CAZy database covers 4623 genomes in the following kingdoms they are: bacteria (3946), archaea (220), eukaryota (180) and viruses (277) [16].

4.3 Fungal Oxidative Lignin Enzymes (FOLy)

When compared to other microorganisms, fungi are the most efficient lignin degraders. Fungi secrete a wide range of extra and intracellular enzymes for the degradation of lignin. Lignin degradation by fungi is a significant step during carbon recycling and for maintaining terrestrial ecosystems. Thus, understanding the fungal enzymes involved in the breakdown of lignin is important. FOLy database was developed to classify the enzymes involved in the breakdown of lignin, by retrieving publicly available information from GenBank, Uniprot PDB, EMP PMD, and Pubmed [18]. The structure of FOLy is similar to that of Carbohydrate Active Enzyme (CAZy) [16]. Degradation of carbohydrates by enzymes is dependent on cocktails of highly specific extracellular enzymes for breaking glycosidic bonds. While lignin depolymerization makes use of various extracellular oxidative enzymes, which are responsible for generating highly reactive free radicals that cause cleavage of carbon-carbon, and inter unit ether bonds. FOLy has classified

lignin breaking enzymes into two major classes as (a) Lignin Oxidizing (LO) enzymes and (b) Lignin degrading auxiliary enzymes (LDA's), based on their potential involvement in lignin breakdown [18].

4.4 Lignin Oxidizing Enzymes (LO)

Non-specificity and high oxidation potential are the main attributes of lignin oxidizing enzymes. Lignin oxidizing enzymes are categorized into three classes LO1 (Laccases), LO2 (Lignin peroxidases, Manganese peroxidases, Versatile peroxidases and Chloroperoxidases) and LO3 (Cellobiose dehydrogenase) (Fig. 4.1). The most thoroughly studied fungal enzymes involved in lignin attack are described below:

4.4.1 Laccases (EC 1.10.3.2, Benzenediol: Oxygen Oxidoreductase)

Laccases represents the largest sub group of blue multicopper oxidases (MCO) and are widely distributed among eukaryotes (fungi, plants) prokaryotes (bacteria) [22] They perform varied functions based on the source organism [22]. Laccase was first discovered in the sap of the Japanese lacquer tree *Rhus vernicifera* [23] and then it was also demonstrated in fungi [24]. Although laccases were discovered during early nineteenth century they have received much attention during the last five

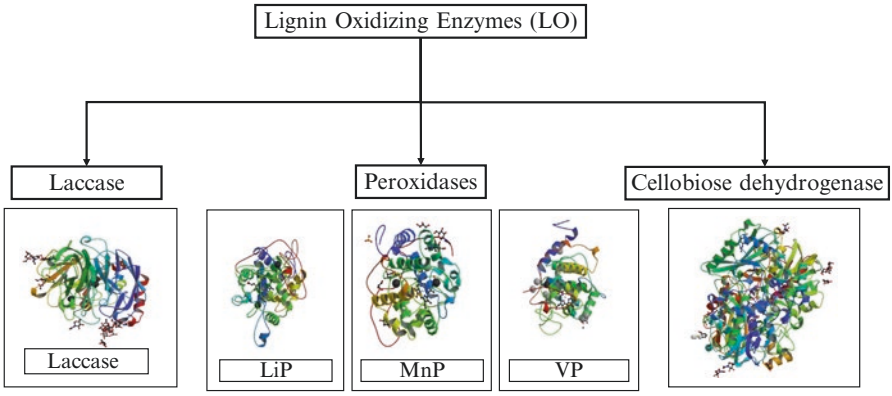

Fig. 4.1 Schematic representation of different lignin oxidizing enzymes namely, laccases (PDB ID: 3FPX), lignin peroxidase (LiP) (PDB ID: 1B85) [19], manganese peroxidase (MnP) (PDB ID: 1YYD) [20], versatile peroxidase (VP) (PDB ID: 3FKG), cellobiose dehydrogenase (PDB ID: 1KDG) [21]. All the enzyme structures were obtained from the PDB RCSB repository

decades for their application to biofuel and biorefinery fields. The involvement of laccase in the degradation of wood by fungal groups such as basidiomycetes, ascomycetes has attracted scientific communities to study the structure, function and mechanisms of laccases [25]. Many fungal species belonging to the basidiomycetes phylum such as *Abortiporus biennis, Agaricus bisporus, Agaricus brunnescens, Armillaria mellea, Aspergillus nidulans, Botrytis cinerea, Ceriporiopsis subvermispora, Ganoderma lucidum, Lentinus edodes, Myceliophthora thermophile, Neurospora crassa, Penicillium crysogenum*, *Phanerochaete chrysosporium, Phlebia brevispora, Phlebia radiata, Pleurotus erygii, Pleurotus ostreatus, Pleurotus sojar-caju Polyporus species, Rhizoctonia Solani, Trametes hirsuta, Trametes versicolor and Trichoderma* were reported to secrete laccase [26]. Laccases are widely studied for two major functions (a) there role in lignin polymerization (lignification) in plants, (b) lignin depolymerization by fungi [27]. The contrasting role of laccases on lignin depolymerization was proved in vitro by Hatakka 1994 and Youn et al. 1995, showing the oxidative reaction of laccases on lignin, resulting in loss of an electron from phenolic hydroxyl groups of lignin resulting in phenoxy radicals [28, 29]. These studies have also showed that these radicals can spontaneously reorganize leading to the cleavage of alkyl side chains of polymer. At the same time, the polymerizing activity of the laccase might result in the polymerization of low molecular weight compounds [26]. These studies suggested that lignin degradation by fungi in nature occurs by the synergistic effect of other lignin degrading enzymes and non-enzymatic components which establishes a balanced environment between lignin depolymerization and enzymatic polymerization [26]. Although studies have reported the involvement of laccases in both lignin polymerization and depolymerization, the exact role of laccases and other partnering enzymes in the degradation and modification of lignin were still under investigation [26, 27]. Apart from wood decay, laccases play important role in fungal physiological processes such as morphogenesis, fungal plant pathogen/host interactions, stress defense and lignin degradation [26, 30]. In fungi, laccases are expressed during different stages of fungal development (morphogenesis, growth of rhizomorphs, sporulation, pathogenesis and virulence). According to Leatham and Stahmann 1981, increased laccase activity was observed in the developing fruiting bodies of *Lentinus edodes* (a commercially cultivable mushroom) [31]. The role of laccases on mushroom development was proved by Ikegaya et al. (1993), in this study the developing fruiting bodies of *L. edodes* were treated with diethyldithiocarbamate (a potential inhibitor of laccase) which resulted in the decreased growth of *L. edodes* fruiting bodies, thus proving the role of laccase in fungal development [32]. A similar study was conducted on *Armillaria mellea* by Worrall et al. (1986) which showed the requirement of laccase for the development and growth of rhizomorphs [33]. Laccases are also involved in imparting specific virulence properties to the fungi, *Botrytis cinerea* (common plant infecting fungi) secretes laccases which causes infection in some plants especially carrot and cucumber by triggering plant toxins such as cucurbitacins and tetracyclic triterpenoids. However, the virulence of these laccases was inhibited in EDTA pretreated plant tissues [34]. Thus fungal laccases play three major functions: lignin degradation, detoxification and pigment formation. Industrially laccases are important in paper and pulp, bio bleaching, textile industries etc.

Structure Several X-ray crystallography studies were conducted to determine the structural properties of laccases (Table 4.2), however in this chapter we are focusing on *Trametes versicolor* laccase. The structural analysis of laccase isolated from *Trametes versicolor* was first done by Klaus Pointek et al. (2002) [35]. Laccase is a monomeric protein ordered in three sequentially arranged domains with dimensions ranging $65 \times 55 \times 45$ Å^3, each domain consists of a β-barrel shaped architecture which is similar to other blue copper proteins such as azurin or plastocyanin [35]. With each domain different from the other domains in their structural composition. First domain comprises two four-stranded β-sheets and four 3_{10}-helices, of which three acts as a connecting peptide between β-strands and one helix forms the segments between first and second domains. The second domain consists of one six stranded and one five stranded β-sheets, with three 3_{10}-helices peptides connecting the individual β-strands and domains 1 and 3. A 3_{10}-helix forms a 40 amino acid long extended loop region between domains 2 and 3. The third domain contains two five stranded and a two stranded β-sheet, which together form a β-barrel. The β-barrel together with an α-helix and a β-turn, forms a cavity for a type-I copper. Compared to the other two domains, the third domain has the highest helical content with one 3_{10}-helix and two α-helices situated in between the connecting regions of different β-sheets. The completion of the protein fold involves the C-terminal end of domain 3 and three sequentially arranged α-helices. Two disulfide bridges (Cys85-Cys488 and Cys117-Cys205) were reported which connects domain 1 and 2 and stabilizes a 13 amino acid residue α-helix. An oxygen reducing site is present at the T2/T3 cluster which accesses the solvent through two channels, leading to type-III copper and to type-II copper sites. The type-II copper site is more exposed and easily altered, when compared to the other two copper sites present near the T3 site. Actually T2 copper site is deficient in copper in the copper depleted forms of both laccase and ascorbate oxidase [36, 62]. Electrostatic potential studies of *Trametes versicolor* laccase shows that it possess a high negative charge, which suggests the specific binding of the substrate to the negatively charged cavity near the T1 copper site. Negative charge occurring at binding site imparts functional significance to the enzyme by imparting stability to the radical cation products formed during catalytic cycle. The two channels near the copper sites provide access to molecular oxygen and allow water release from the T2/T3 cluster. At the same time a conserved His-Cys-His tripeptide is associated with the electron transfer pathway between the T1 copper and the trinuclear cluster. A two site ping pong bi-bi reaction mechanism was proposed for the catalytic mechanism of laccase enzyme [63], which means that products are released before binding of new substrates.

Mechanism of Action Laccases use their distinctive redox ability of copper ions for catalyzing the oxidation of various aromatic substrates concurrently reducing the molecular oxygen to water [64]. Laccases are able to catalyze direct oxidation of ortho, para-diphenols, aminophenols, polyphenols, polyamines, aryl diamines and also some inorganic ion [26, 65–69]. Laccases depends on copper (Cu) for their catalytic action, based on the number of copper ions laccases can be classified as dimeric or tetrameric glycoproteins. In addition, based on the types of copper ion centers they are classified as: (a) Type-I (blue copper center) (b) Type-II (normal

Table 4.2 Lists the catalytic mechanism and structural studies of different lignin oxidizing enzymes

Enzyme, FOLy Class	Catalytic mechanism	Structural studies, references
Laccase (LO1) (EC 1.10.3.2)	$4\ \text{benzendiol} + H_2O_2 \rightarrow 4\ \text{benzosemiquinone} + 2H_2O$	*Trametes versicolor* [35]
		Coprinus cinereus [36]
		Melanocarpus albomyces [37]
		Cerrena maxima [38]
		Thielavia arenaria [39]
		Lentinus tigrinus [40]
Lignin Peroxidase ((LO2) (EC 1.11.1.14)	LiP oxidizes alkyl side chains and benzyl alcohol, It is involved in breakdown of C–C side chains and aromatic rings of lignin	*Trametes cervina* [41]
		Phanerochaete chrysosporium [42, 43] [44–48]
Manganese Peroxidase (LO2) (EC 1.11.1.13)	MnP's catalytic mechanism is dependent on hydrogen peroxide and Mn^{2+} ions.	*Phanerochaete chrysosporium* [20, 49–52]
Versatile Peroxidase (LO2) (EC 1.11.1.16)	VP has substrate specificity features similar to that of MnP and LiP	*Pleurotus eryngii* [53–57]
Cellobiose Dehydrogenase (LO2) (EC 1.1.99.18)	CDH catalyzed reactions [58]	*Phanerochaete chrysosporium* [21, 59–61]
	$\text{Cellobiose} + 2\,Fe^{3+} \rightarrow \text{Cellobionolactone} + 2\,Fe^{2+}$	
	$\text{Cellobiose} + + O_2 \rightarrow \text{Cellobionolactone} + H_2O_2$	
	$Fe^{2+} + H_2O_2 \xrightarrow{(\text{Spontaneous reaction})} Fe^{3+} + OH\ + OH*$	

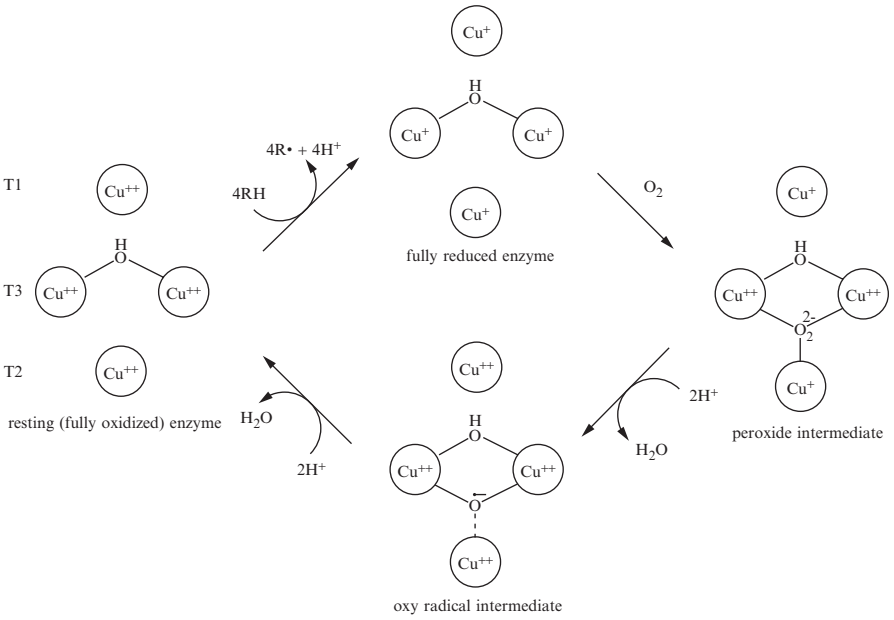

Fig. 4.2 Catalytic cycle of laccase (Reprinted with permission from Ref [9], Copyright © 2008 Springer Science + Business Media B.V)

copper center) (c) Type-III (coupled binuclear copper center) that differ in their characteristic electronic paramagnetic resonance (EPR) signals [70, 71]. Type-I copper coordinates with four amino acids as ligands: two histidines, one cysteine and one methionine. Type-I copper containing laccases are generally a deep blue color, which can be detected by its absorbance at 600 nm wavelength. However, laccases which fail to absorb at 600 nm were reported in *Pleurotus ostreatus* (called white laccase) [72] *Panus tirinus* (called yellow laccases) [73]. Type-II copper coordinates with two histidine and water as ligands, Type-III copper coordinates with three histidines and a hydroxyl bridge which imparts strong anti-ferromagnetic coupling between the type-III copper atoms [35]. Type-II copper atoms do not absorb in the visible spectrum, while type-III copper atoms have an electron absorption at a wavelength of 330 nm. Based on the structural properties of type of copper ions laccases are divided into high and low redox potential enzymes. Bacteria and plants secrete low redox potential laccases, whereas white rot fungi and some basidiomycetes secrete high-redox potential laccases [74, 75].

Different copper centers present in the laccase participate and complete the enzymatic reaction. Unlike peroxidases laccases does not require hydrogen peroxide for the oxidation of monolignols. Enzyme catalysis can be divided into three main stages: the copper ion of type-I is reduced by the reducing substrate followed by internal electron transfer between the type-I, type-II and type-III Cu clusters [22]. Finally the reduction of oxygen takes place at the type-II and III Cu's resulting in water formation (Fig. 4.2). *In vitro* lignin degradation by laccase primarily oxidizes

phenolic hydroxyl groups of lignin to form phenoxy radicals which further reorganize to cleave the alkyl side chains. Laccase can degrade β-1 and β-O-4 dimer linkages between Cα-Cβ and cause Cα oxidation and aryl-alkyl cleavages [22]. Thus the generated reactive radicals further release monomers by breaking down covalent bonds [76]. Due to the steric hindrance of laccase it cannot directly contact large polymers, thus small organic compounds or metals such as veratryl alcohol, manganese and 3-hydroxy anthranilic acid are oxidized and further activated to mediate radical catalyzed depolymerization of lignin [9, 76].

4.4.2 Peroxidases (EC:1.11.1.x)

Peroxidases are large group of enzymes widely distributed among plants, animals and microbes. Peroxidases play a wide variety of activities based on the source of the organism. Peroxidases are involved in several physiological processes such as plants defense mechanisms (response to pathogens), wound healing, auxin catabolism, lignification and suberization [77]. Microbes such as fungi and bacteria are well known for their ability of delignification which is efficiently fulfilled by the different types of peroxidases such as (LiP, MnP and VP). Peroxidases can also efficiently decolorize synthetic dyes and bioremediation of waste water and degradation of several toxic chemicals such as phenolic contaminants, polychlorinated biphenyls, chlorinated alkanes and alkenes, chlorinated dioxins, chlorinated insecticides and removal of endocrine disruptive chemicals etc, thus playing variety of roles in the environment [78]. Molecular structures of lignin degrading peroxidases share several common characteristics such as [79], Ligninolytic peroxidases generally contain a haem cofactor located internally in a cavity (haem pocket), which is connected to the protein by two small access channels [79–83]. Larger channel are common among all haem peroxidases, they are required for the hydrogen peroxide to reach the haem and react with (Fe^{+3}) forming an activated two electron enzyme form called compound I [79–83]. The entrance of this channel forms the substrate binding site in some peroxidases. A second channel extends to the heme propionate substrate where some specific lignolytic enzymes oxidize Mn^{2+} and Mn^{3+} which acts a diffusible oxidizers of phenolic lignin and other organic molecules [79–83]. In this section we will be focusing on the delignification mechanisms of lignin peroxidases, manganese peroxidases, and versatile peroxidase.

4.4.3 Lignin Peroxidases (E.C. 1.11.1.14)

Lignin peroxidases (LiP) the most studied lignin depolymerizing enzymes, LiP was first discovered in the extracellular medium of *P. chrysosporium* under nitrogen limited conditions [84]. Similar to classic peroxidases, LiP are dependent on

hydrogen peroxide. The overall reaction mechanism of LiP is 1,2-bis(3,4-dimethoxyphenyl) propane-1,3-diol + H_2O_2 ⇌ 3,4-dimethoxybenzaldehyde + 1-(3,4-dimethoxyphenyl)ethane- 1,2-diol + H_2O [9]. LiP can oxidize a wide range of phenolic compounds, organic compounds and also different lignin model non-phenolic compounds by using hydrogen peroxide with a redox potential up to 1.4 V, thus showing its non-specificity towards substrates [85].

Structure Structure of *P. chrysosporium* lignin peroxidase (LiP) was determined using protein crystallography by Edward, et al. (1992). These studies revealed that fungal LiPs are globular and mostly helical glycoproteins with a molecular size of 38-46 kDa with 343–344 amino acids depending on the isozyme with a reduction potential exceeding 1.4 V [9, 42]. Compared to other lignolytic peroxidases it has a characteristic low optimum pH 3 with pI values ranging between 3.2 and 4.0 [9]. LiP contains several *N*- and *O*- glycosylation sites, it was reported that *N*-glycosylated sites (Asn257) and *O*-glycosylated site (Ser334 and Thr320) were clustered at the end of the proximal domain [43]. LiP is a globular protein with proximal C-terminal and distal N-terminal domains, the C-terminal segment of about 50 amino acids is extended to pass through the surface with less contact to the protein core [9]. LiP consists of eight major and eight minor α-helices and limited β structure in the proximal domains, it also has eight Cys residues forming disulfide bonds. The calcium binding site present in each domain is involved in maintaining the topology of the active site. The peroxide binding site is located on the distal end of the heme with an extended channel towards the exterior of the protein. The negative charge developed as a result of peroxide cleavage is stabilized by the Arg43 residue, it also stabilizes the ferryl oxygen of compound I. At the same time His47 with Asn82 present on the distal end of the enzyme acts as a proton acceptor for the bound peroxide substrate [9]. The overall protein fold of LiP is similar to other typical haem peroxidases such as cytochrome c peroxidase, manganese peroxidase, horseradish peroxidase [42]. The haem moiety divides the protein structure of LiP into a proximal and a distal domain. The haem moiety is hidden inside the protein with limited access to the outer medium by a small channel [43]. Thus the crystal structure of LiP shows that the haem access channel is not sufficient to allow entry to large polymers like lignin, however this is the only channel to form a suitable binding site for the attachment of small molecule substrates [43]. Protein modeling studies have confirmed its suitability for binding of veratryl alcohol, however the exact binding site of veratryl alcohol was not determined. LiP possess two substrate binding sites for veratryl alcohol (VA), the first one is Trp 171 and the second one is the anionic substrate oxidation site [43]. To find the binding site of the VA on LiP, the molecular docking study was conducted by chemically modifying the surface of LiP enzyme with 1-ethyl-3-(3-dimethylaminopropyl) carbodiimide (EDC) in the presence and absence of 2-aminoethanesulfonic acid for the introduction of N-acyl-urea groups in place of carboxyl groups. LiP was also modified by N-bromosuccinimide (NBS) to yield a Trp modified enzyme [86]. From these studies it was shown that VA probably binds to Trp171 or its surrounding area as a reducing substrate and enzyme bound mediator. At the same time it has been suggested that VA binds at different

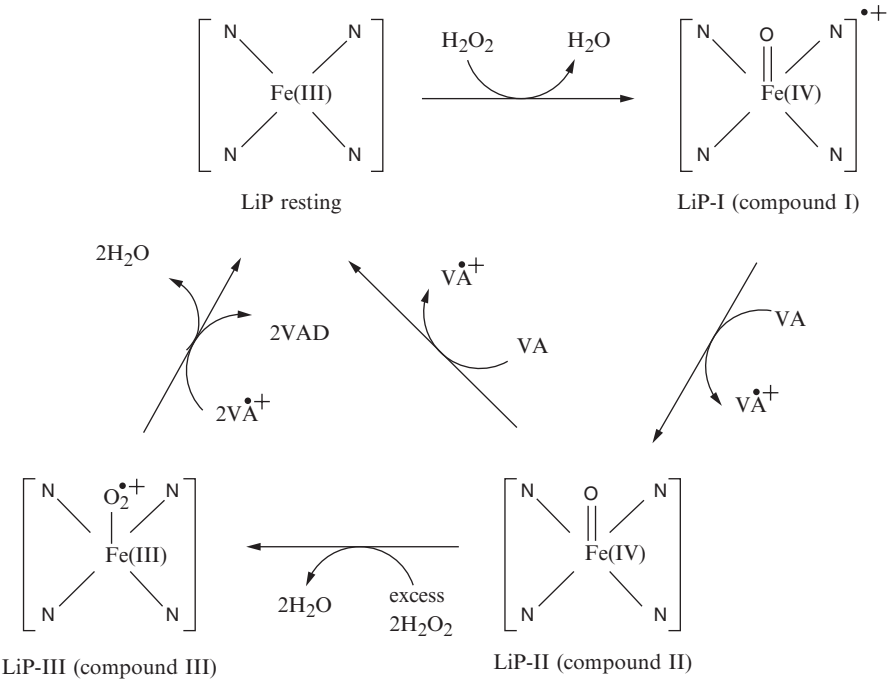

Fig. 4.3 Catalytic cycle of lignin peroxidase (Reprinted with permission from Ref [9], Copyright © 2008 Springer Science + Business Media B.V)

locations when it reacts with LiP compound III* for the reverse reaction. The major difficulty in determination of the VA binding site is the lack of inhibitors causing classical inhibition patterns like competitive or non-competitive inhibitions. Thus, studies should be conducted by using X-ray crystallography and NMR methods for the determination of the LiP binding site for VA [9, 86].

Mechanism Lignin peroxidase resembles horse radish peroxidase (a classical peroxidase highly studied) by containing Fe (III) as a cofactor which is pentacoordinated to four heme tetrapyrrole nitrogens and to a histidine residue [87]. Lignin peroxidases are dependent on H_2O_2 for their reaction. H_2O_2 oxidize LiP resulting a two electron-oxidized intermediate (Compound I) in which iron is present as Fe (IV) leaving a free radical on the tetrapyrrole ring or on a nearby amino acid. Compound I then oxidizes a donor substrate to form a second intermediate (Compound II) and a substrate free radical (Fig. 4.3) [87]. Later reduction of the enzyme to its resting state can be accomplished either by the same substrate molecule or with a second substrate molecule by giving off substrate-free radical [87]. An important functional difference between LiP and other classical peroxidases is that lignin peroxidases can oxidize aromatic rings that are moderately activated by electron donating substituents, at the same time classical peroxidases act only on strongly activated aromatic substrates. Therefore, LiP and horseradish peroxidase can oxidize 1, 2, 4, 5-tetra-

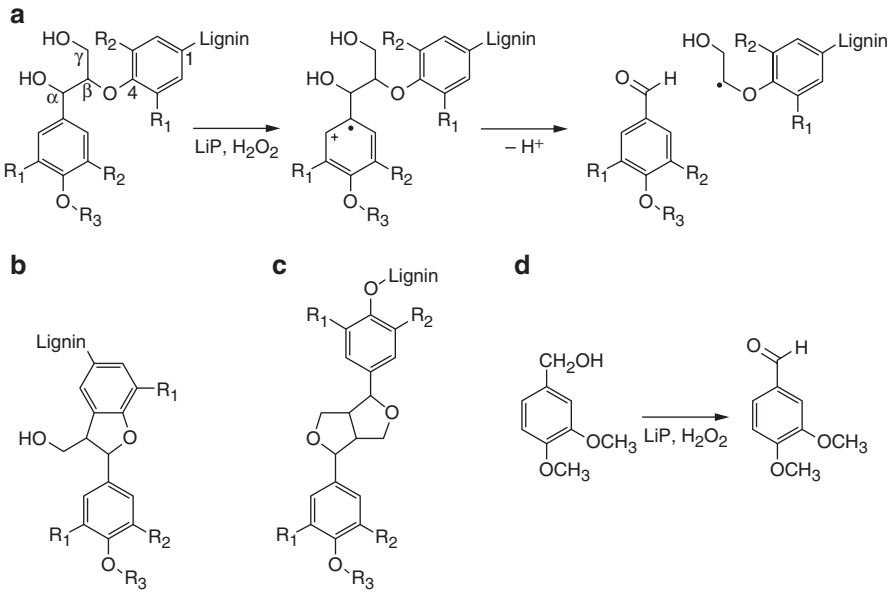

Fig. 4.4 Chemical structures and reactions discussed in the text. (**a**) The principal β-O-4 structure of lignin and pathway for its C_α–C_β cleavage by LiP. (**b**) A phenylcoumaran lignin structure. (**c**) A resinol lignin structure. (**d**) LiP-catalyzed oxidation of the fungal metabolite veratryl alcohol. Gymnosperms contain lignin's in which most subunits have $R_1 = OCH_3$ and $R_2 = H$. Angiosperm lignin's also contain these structures, but have in addition subunits in which $R_1 = OCH_3$ and $R_2 = OCH_3$. Grass lignin's contain both types of structures but have in addition some subunits in which $R_1 = H$ and $R_2 = H$. These nonmethoxylated lignin structures are more difficult to oxidize than those that contain one or two methoxyl groups. In the predominating nonphenolic structures of lignin, R_3 = lignin, whereas $R_3 = H$ in the minor phenolic structures (Reprinted with permission from Ref [87], Copyright © 2008, Elsevier)

methoxybenzene, phenols and anilines, at the same time LiP are capable of abstracting an electron from aromatics that carry only two or three ether like the major nonphenolic structures of lignin [88]. Primary products of this oxidation are temporary cation radical intermediates which certainly breakdown. Majorly Cα-Cβ bonds of propyl side chains are broken down to give benzaldehydes which are the precursors of benzoic acid molecules, these benzoic acid molecules are mainly observed in lignin decaying white rot fungi (Fig. 4.4) [89]. The unusual activity of lignin peroxidases is due to two structural differences, an electron-deficient iron atom in the porphyrin compared to classical peroxidases which makes LiP a stronger oxidant [90] and an invariant Trp171 in the isozyme of LiPA. This residue is present on the enzyme surface and is known to participate in a wide range electron transfers from aromatic substrates since they cannot contact the oxidized haem directly [91]. This important feature of LiP is responsible for oxidizing complex lignin and its related substrates directly. This function of Trp171 in LiPA was proved by a site directed mutagenesis in which the Trp171 was replaced by serine, which resulted in the loss of activity [92]. It was shown that the efficiency of LiP catalyzed oxidation of lignin

molecules markedly decreases with an increase in size of the lignin molecule. LiP catalyzed oxidation of lignin trimers was found to be only 4 % of the rate of oxidation of a monomer model [93]. Oxidation of lignin molecules by LiP takes place in the presence of veratryl alcohol, and the role of VA in oxidation by LiP are given below [87]. Studies have showed that the VA cation radical oxidizes has a long half-life of 40 ms even at acidic conditions [94, 95]. VA is the substrate of LiP. It was suggested that the VA cation radical oxidizes lignin molecules at remote locations [96]. VA acts as an efficient electron donor to protect LiP from oxidative inactivation by hydrogen peroxide. As LiP oxidizes large and complex lignin substrates, which is a slow reaction, VA prevents oxidization of LiP [97]. VA is also essential for the reduction of LiP compound II. Compound I is reduced by non-methoxylated lignin structures. As these lignin structures are difficult to oxidize since they carry only one electron donating ether group. Compound II of LiP is a comparatively weaker oxidant than compound I [98].

4.4.4 Manganese Peroxidases (EC 1.11.1.13)

Wood decaying white rot fungus and other litter decomposing fungi efficiently degrade lignin in wood. These fungi secrete several non-specific oxidoreductases, among them manganese peroxidase plays an important role [99]. Manganese peroxidase (MnP) was first discovered in *P. chrysosporium* two decades ago [100, 101], however it received less attention then lignin peroxidase in beginning. Later it was found that LiP is not produced by all white rot fungi [28, 102, 103]. Production of MnP is limited only to basidiomycetes. Mainly two ecophysiological groups of fungi i.e. wood degrading fungi causing white rot and soil litter decomposing fungi secrete manganese peroxidase [103]. Wood decaying fungi belonging to families such as *Meruliaceae, Coriolaceae, Polyporaceae* and soil litter decomposing fungi such as *Strophoriaceae, Tricholomataceae* are known fungal families, which secrete MnP. Some prominent MnP producing fungi are *Abortiporus biennis, Agaricus bisporus, Armillaria mellea, Auricularia sp. M37, Bjerkandera adusta, Ceriporiopsis subvermispora, Coriolopsis polyzona, Dichomitus squalens, Ganoderma lucidum, Heterobasidion annosum, Hypholoma fasciculare, Lentinula (Lentinus) edodes, Panus tigrinus, Phaeolus schweinitzii, Phallus impudicus*, *Phanerochaete chrysosporium, Phanerochaete sordida, Phlebia brevispora, Phlebia radiata, Pleurotus enryngii, Pleurotus sajor-caju, Stropharia aeruginosa, Stropharia coronilla, Trametes hirsuta, Trametes versicolor* [99].

Structure The enzyme mechanism of MnP is similar to that of classical haem containing peroxidases, but this enzyme is unique by having Mn^{+2} as a reducing substrate [49]. Crystal structure of *P. chrysosporium* MnP was demonstrated by Sundaramoorthy et al. (1994). MnP is an acidic glycoprotein with pI near to 4.5, it is often produced as a sequence of isozymes which are differentially regulated by different genes [104]. It contains one molecule of heme in iron protoporhyrin IX, showing a maximal activity at Mn (II) with concentrations above 100 μM [100]. The

enzyme oxidizes Mn from Mn^{+2} to Mn^{+3}, it forms complexes with oxalate and acts as a diffusible redox mediator for the oxidization of lignin and other phenolic compounds. MnP is a haem containing glycoprotein with a molecular weight ranging between 38 and 62.5 kDa, however most of the purified enzymes have molecular weights around 45 kDa. About 43 % of the amino acid sequence of MnP is identical to LiP, overall protein folding of MnP is similar to that of other plant and fungal peroxidases [49, 50]. MnP consists of two domains and haem submerged between these domains, similar to that of LiP. MnP enzyme consists of ten major and one minor helix similar to that of LiP. Eight minor helices are present in MnP of which two minor helices are similar to that of LiP all are in the 3_{10} helical confirmation. It contains five disulfide bonds of which Cys^{3}-Cys^{15}, Cys^{33}-Cys^{117}, Cys^{14}-Cys^{289}, Cys^{253}-Cys^{319} are similar to that of LiP and only one disulfide bond is unique to MnP [49, 50]. The unique disulfide bond Cys^{341}-Cys^{348} is part of the long C-terminal tail in MnP which is partially responsible for forcing C-terminus away from the main body of the protein, which might be involved in manganese binding site formation. Arg^{42} and His^{46} on the distal domain of MnP form the peroxide binding pocket, and histidine in the distal domain is required for the formation of compound I by acting as acid base catalyst [20, 49]. Superposition studies conducted on LiP and MnP have shown few significant facts such as differences occurring at the insertion sites of these enzymes. In LiP, the C-terminus lies between two heme propionate groups while in MnP the C-terminus is separated from the heme by the combined effects of a 7-residue insertion (Leu^{228}-Thr^{234}) in the loop between the G and H helices, Arg^{177}, Glu^{35}, and the Cys^{341}-Cys^{348} disulfide bond [20, 50]. It was also reported that the His46 and Asn80 residues present in the distal end are hydrogen bonded, which is required for $N\varepsilon_2$ of His46 to accept proton from the peroxide during acid-base catalysis. Similarly the hydrogen bond between His173 and Asp242 involved in increasing the anionic character of the ligand and further stabilizing the oxyferric iron in MnP-I. The cation binding site present on the surface of the protein is formed by several interactions of Mn (II) with the carboxylate oxygen groups of Glu35, Glu39, and Asp179, the heme propionate oxygen and two water. The oxygens impart flexibility and facilitate the binding of a wide range of metal ions. MnP also contains of two calcium ions bound tightly on the proximal and distal side chains of the heme that are involved in maintaining the thermal stability of the active site of MnP [9, 20, 49, 50].

Mechanism MnP is different from other peroxidases as it uses Mn (II) as the reducing substrate. MnP oxidizes Mn (II) to Mn (III), which then catalyzes the oxidation of a wide range of monomeric phenols, lignin model phenolic compounds and dyes [100, 105, 106]. The reaction mechanism of MnP proceeds as: first oxidation of Mn (II) by compound I (MnP-I), followed by oxidation of compound II (MnP-II) yielding Mn (III). MnP is a strong oxidizing agent like LiP, it cannot oxidize nonphenolic lignin related compounds because it lacks the invariant Trp171 residue which is required for electron transfer to aromatic substrates [87]. MnP has a manganese binding site which contains many acidic amino acids and also a heme propionate group. Thus one electron transfers to compound I of MnP takes place from bound Mn^{+2}. Further Mn^{+3} is released from the active site in presence of the

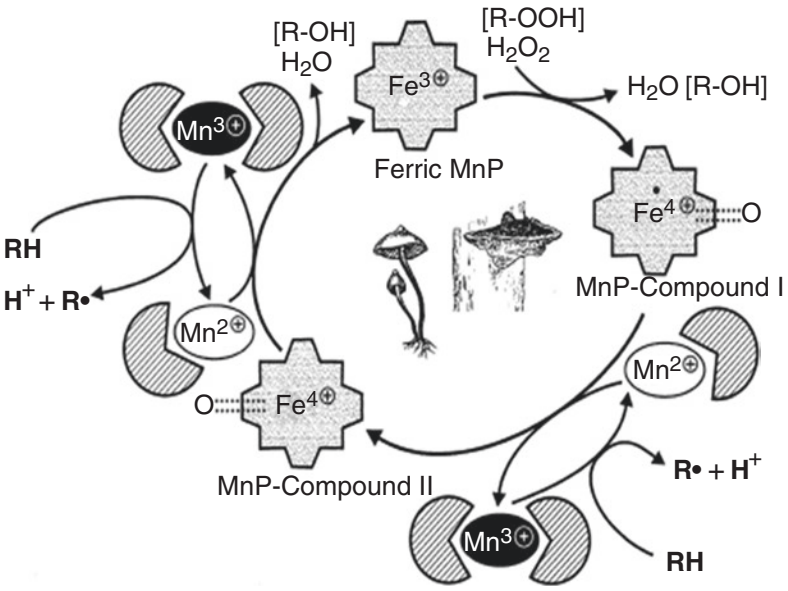

Fig. 4.5 Catalytic cycle of manganese peroxidase (Reprinted with permission from Ref [99], Copyright © 2002, Elsevier)

bidentate chelators such as oxalate, which helps prevent the disproportionation to Mn^{+2} and insoluble Mn^{+4}. This reaction is required for the transfer of oxidizing power of MnP to Mn^{3+}, which diffuses into the lignified cell wall thus attacking it from inside [87]. An important feature of MnP is to oxidize the low permeable lignocellulose network making it different from other peroxidases [9]. Chelators such as oxalate increase the electron density on Mn^{+3} which makes it a weak oxidant, thus Mn^{+3} organic acid chelates produced by MnP cannot oxidize the nonphenolic substrates of lignin. Mn^{+3} chelates cannot cause extensive lignolysis as they can only attack rare phenolic structures of lignin, which often are the end groups of lignin. The catalytic cycle of MnP begins with the binding of hydrogen peroxide or an organic peroxide to the native ferric enzyme resulting in the formation of an iron-peroxide complex (Fig. 4.5). Further the breakdown of the oxygen-oxygen peroxide bond depends on a 2-electron transfer reaction from the heme resulting in the formation of MnP compound I (i.e. a Fe^{4+}-oxo-porphyrin radical complex). The dioxygen bond is cleaved resulting in removal of water and further reduction proceeds via MnP compound II. The Mn^{2+} ion (monochelated) donates one electron to the porphyrin intermediate and is oxidized to Mn^{3+}. Similarly compound II is reduced by releasing another Mn^{3+} and a second water molecule, thus leading to the resting state of the enzyme (Fig. 4.5) [107–109].

The oxidation of phenolic compounds by MnP occurs by Mn (III) chelator complexes, which diffuses and catalyzes one electron oxidation of phenolic compounds producing a phenoxy radical intermediate. The phenoxy radical intermediate under-

goes bond cleavages, rearrangements and degradation of compounds non-enzymatically to produce different breakdown products [106, 110, 111]. In contrast unchelated Mn (III) causes the formation of reactive radicals as second mediators for the oxidation of non-phenolic compounds. Oxidation of non-phenolic compounds by MnP is different from LiP, as LiP oxidizes by abstracting electrons from the aromatic ring resulting in a radical cation. In presence of thiols like glutathione, Mn (III) causes the oxidation of benzyl alcohol and diarylpropane structures to their corresponding aldehydes [112, 113].

4.4.5 Versatile Peroxidases

Versatile peroxidases a new family of lignolytic peroxidases were reported for the first time in *P. chrysosporium* along with other lignolytic enzymes such as LiP and MnP [79]. Several fungi belonging to genera such as *Pleurotus, Bjerkandera, Lepista, Panus* and *Trametes* species were reported to produce versatile peroxidase (VP). Versatile peroxidase have important properties which combines the substrate specificity characteristics of the three fungal peroxidases such as manganese peroxidase, lignin peroxidase and Coprinus cinereus peroxidase [79]. Two well-known studies have revealed the occurrence of versatile peroxidases in nature, in the first study a Mn^{2+} binding site was introduced into the LiP of *P. chrysosporium* by site directed mutagenesis, the resulting enzyme had MnP activity [114]. In the second study a tryptophan residue similar to that in LiP was introduced into the MnP of *P. chrysosporium* and the enzyme acquired LiP activity [115]. Versatile peroxidase coding genes were first cloned and sequenced from *Pleurotus eryngii*. Studies of the catalytic properties of VP suggested that they were due to its hybrid molecular construction combining different oxidation and substrate binding sites [116, 117].

Structure Crystallographic studies conducted by Boada et al. (2005) showed that the structures of VP and its variant W164S are very similar. A total of 319 (VP) and 320 (W164S) amino acid residues along with heme and other cations were shown in the structural studies [53, 79]. The VP structure includes 11 α-helices (Ala12-Asn27, Glu36-Ala49, Ser64-Glu72, Ile81-Lys94, Ala99-Ser112, Val145-Ala155, Pro159-Ile171, Gln196-Glu200, Gln229-Arg236, Ala241-Ser246 and Gln251-Ala266), four disulphide bridges (Cys3- Cys15, Cys14-Cys278, Cys34-Cys114 and Cys242- Cys307) and two structural Ca^{2+} ions [79]. The Mn^{2+} binding site of VP contains three amino acid residues: Glu36, Glu40 and Asp175, The binding site is formed by the carboxylate groups of these amino acids and also the carboxylate group of the heme propionate. It is known that oxidation of compounds by VP occurs through LRET (Long Range Electron Transfer) pathways, structural studies reveal that three putative LRET pathways were present in the VPL isoenzyme for the oxidation of aromatic compounds. They are (i) His232-Asp231 via backbone atoms and H-bond from the carboxylate of Asp231 to the side chains of the proximal His169, (ii) backbone atoms between Trp164 and Leu165 and a van der Waals

contact between C^{β} of Leu165 to the methyl group C of the heme, and (iii) Pro/His76-Ala77– Asn78 via backbone atoms and a H-bond from the side-chain oxygen atom of Asn78 to the distal His47 [79]. From site directed mutagenesis studies of the LRET pathways clearly show that the Trp164 pathway of VP is involved in the oxidation of high redox potential compounds such as veratryl alcohol and reactive black 5. Studies also showed that oxidation of veratryl alcohol and reactive black 5 and other high redox potential compounds by VP involves electron transfer from activated VP* through the Trp164 side chain to the backbone and then to the side chain of Leu165, whose Cβ is 3.66 A ° from the carbon of the methyl-C of heme (2.37 A° hydrogen distance) [79]. A comparison with LiP isoenzymes shows either Met (LiPH8) or Leu (LiPH2) are homologous with VP Leu165. Eight neighboring residues with three conserved regions are shown to illustrate the differences between the structures, as well as the position of the proximal histidine residues, whose Nε atoms act as ligand of heme iron at 2.11 A° in VP and 2.15 A° in LiP [53–56, 79].

Mechanism Basic features of versatile peroxidase are similar to those of all other classical peroxidases, however it is unique as far as the substrates that it is able to oxidize. A complete catalytic cycle combining those of other fungal peroxidases such as LiP and MnP was proposed by Ruiz-Duenas et al. Similar to LiP, versatile peroxidase also initiates the LRET pathway (Long range electron transfer) at an exposed tryptophan residue [79, 118]. Studies have examined the catalytic mechanism of VP using veratryl alcohol (reducing substrate) and its transitory states in the catalytic cycle. On reaction with one molecule of hydrogen peroxide the ferric group of VP (resting state) was converted to Compound I (Fe^{4+}-oxo-porphyrin^{+} complex) causing spectral changes (Fig. 4.6) [54, 55, 79]. Compound I oxidizes a molecule of veratryl alcohol resulting in Compound II (Fe^{4+}-oxo), which will further oxidize another molecule of veratryl alcohol further reducing the enzyme back to its resting state [54, 79]. VP can oxidize high redox potential dyes like reactive black 5 (RB5) and also can oxidize low redox potential compounds such as phenolic monomers, simple amines, Mn^{2+} etc [118]. Compared to LiP and MnP the oxidization capacity of VP is higher for phenolic compounds, this ability might be due to its relatively more accessible distal main solvent channel allowing a third lower redox potential substrate oxidation site as in CiP. A research study conducted by Parez-Boada et al. reported that the spectral changes occurring during the oxidation of phenolic compounds by VP shows that VP in its resting state has a higher absorbance at 407 nm. Similarly during charge transfer, the transient states such as Compound I and II have an absorbance at 505 nm and 637 nm respectively [54, 79]. Two major enzymes MnP and VP are known for their ability to oxidize Mn^{2+} to Mn^{3+}, the Mn^{2+} oxidation site of *P. eryngii* VP is similar to that of *P. chrysosporium* MnP. In VP, the Mn^{2+} binding site is formed by the side chains of Glu36, Glu40 and Asp175 located in front of the internal propionate of heme. Carboxylate groups of the amino acids and heme propionate are responsible for Mn^{2+} binding and for succeeding electron transfer to the activated heme of VP compounds I and II. Studies of the VP crystal structure showed a variable orientation of the Glu36, and Glu40 sidechains by interaction with Asp175 [118]. The position of these amino acids in

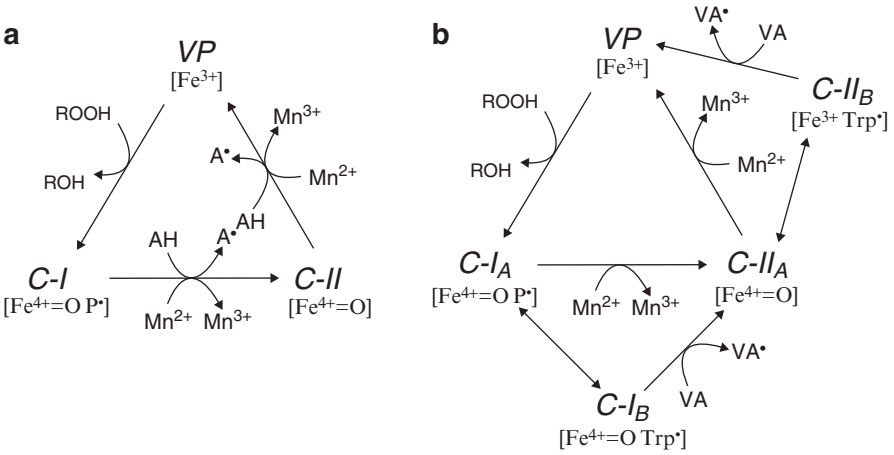

Fig. 4.6 Schemes of VP catalytic cycle. (**a**) Basic cycle described by [116] including two-electron oxidation of the resting peroxidase (VP, containing Fe^{3+}) by hydroperoxide to yield compound I (C-I, containing Fe^{4+}-oxo and porphyrin cation radical), whose reduction in two one-electron reactions results in the intermediate compound II (C-II, containing Fe^{4+}-oxo after porphyrin reduction) and then the resting form of the enzyme. As shown in the cycle, VP can oxidize both: (i) aromatic substrates (AH) to the corresponding radicals (A·); and (ii) Mn^{2+} to Mn^{3+}, the latter acting as a diffusible oxidizer. (**b**) Extended cycle including also compounds I_B (C-I_B, containing Fe^{4+}-oxo and Trp radical) and II_B (C-II_B, containing Fe^{3+} and Trp radical) involved in oxidation of veratryl alcohol (VA) and other high redox potential aromatic compounds (C-I_B and C-II_B are in equilibrium with C-I_A and C-II_A respectively, which correspond to C-I and C-II in (**a**) (other low redox potential aromatic compounds are probably oxidized by both the A and B forms but they are not included for simplicity). The active Trp in C-I_B and C-II_B would be Trp164 (the part of the cycle showing aromatic substrate oxidation would be also applicable to LiP, being Trp171 the active amino acid) (Reprinted with permission from ref [79], Copyright © 2005, Elsevier)

recombinant VP shows an open gate conformation before exposure to Mn^{2+}, thus enabling the oxidation of the Mn^{2+}. At the same time native *P. eryngii* VP shows that the two glutamate side chains are pointed towards the Mn^{2+} corresponding to a closed gate conformation. In this conformation the carboxylate groups of Glu36, Glu40, Asp 175 and the propionate heme groups are at a distance from Mn^{2+}. VP also oxidizes high redox potential substrates similar to LiP (a classic ligninolytic enzyme) through the LRET pathway. This pathway occurs in several redox proteins like cytochrome-c-peroxidase, which oxidizes cytochrome-c on its surface by transferring electrons to tryptophan residues [54, 55, 118]. The LRET pathway was known earlier for its involvement in lignin degradation by different ligninolytic enzymes, thus overcoming steric hindrance which prevent the direct interaction of the heme group and the lignin polymer. Structural studies of VP show that three possible LRET pathways are involved during the oxidation of aromatic substrates by VP [118]. Oxidation of aromatic substrates starts at Trp 164 or His232 of VPL and at His82 or Trp170 of VPS1. VP can also efficiently oxidize low reduction potential compounds like ABTS, p-hydroquinone and 2, 6 dimethoxy phenol. Enzyme kinetics studies have showed that VP has two independent oxidation sites

characterized by high and low specificities. Site directed mutagenesis of VP Trp164 performed by Ruiz-Duenas et al. showed that in Trp164 mutants the high specificity active site was removed while the low specificity site remained intact [55, 118]. Studies have confirmed a similar effect of a W164S mutation on VP oxidation of phenols. Based on these studies we conclude that the catalytic features of VP are due to its hybrid molecular architecture which includes different oxidation sites for Mn2+, high redox potential substrates (aromatic compounds) and low redox potential substrates (phenols and dyes) [55, 118].

4.5 Cellobiose Dehydrogenase

Cellobiose dehydrogenase is an extracellular enzyme involved in carbohydrate metabolism that was shown to be involved in lignin degradation [119, 120]. It was first isolated from an imperfect form of *P. chrysosporium* (*Sporotrichum pulverulentum*) [121]. Cellobiose dehydrogenase is a flavocytochrome enzyme which can oxidize various carbohydrates such as cellobiose (major product of cellulose degradation) and mannobiose (product of mannose degradation) [58]. Several fungi were reported to produce cellobiose dehydrogenase, mostly white rot fungi such as *P. chrysosporium* (*Sporotrichum pulverulentum*), *Trametes versicolor, Pycnoporus cinnabarinus, Polyporus dichrous, Merulius tremellosus, Phlebia radiata, Pleurotus ostreatus* and *Fomes annosus. Coniophora puteana (brown rot fungi)* soft rot fungi, such as *Sporitrichum thermophile (Myceliophthore thermophile), Schizophyllum commune, Humicola insolens, Sclerotium Rolfsii, Chaetomium cellulolyticum*, imperfect soft rot fungi such as *Monilla sitophila, Agaricus bisporus (Mushroom, Stachybotrys (Mold), Cladodporium(Mold)* [121]. CDH degrades cellobiose and mannobiose to lactones by removing two electrons, which can be further transported to electron acceptors such as quinones, phenoxyradicals and dioxygen [58]. In CDH two prosthetic groups, FAD and heme, makes the enzyme suitable for the reduction of one electron acceptors such as radicals and metal ions. CDH has a high specificity for amorphous cellulose and less towards microcrystalline cellulose a unique property among non-hydrolytic enzymes [58]. CDH can produce hydroxyl radicals by reducing Fe^{3+} to Fe^{2+} and O_2 to H_2O_2, These reactive species depolymerize cellulose, xylan and to some extent lignin polymers [58].

Structure A crystallographic study of cellobiose dehydrogenase was performed by Hallberg et al. (2002) [21]. Cellobiose dehydrogenase is a 90 kDa protein consisting of 752 amino acid residues, with a MW of 80 kDa and 10 kDa due to mannose glycosylation [121]. CDH is a monomeric enzyme with a flavin domain containing FAD (60 kDa) and a heme domain (30 kDa) containing a cytochrome b type heme. These two domains are connected by a fifteen amino acid residue linker. The FAD-binding subdomain consists of 205 amino acids, in an α/β type fold containing a six stranded parallel β-pleated sheet which is between three anti parallel β-sheets (β meander) and three α-helices [21]. Its sequence and structural predictions suggests that the ADP binding moiety of the cofactor consists of a βαβ motif, which is usually seen in NAD or FAD dependent enzymes [21]. The F-subdomain also consists of three α-helices

which together form the substructure on one side of the F-subdomain [21]. The substrate binding domain (S-subdomain) consists of 335 amino acid residues forming a central twisted seven stranded β-sheet (Sheet B), also containing three α-helices on one side of the sheet with the active site on the other side. The S-subdomain consists of a relatively long 3_{10} helix and two α-helical regions, finally sheet B forms the bottom of the active site. The beginning of the S-subdomain forms a loop and lid structure that outlines the entrance of the active site and the outer wall of the FAD binding pocket [21]. The heme unit of CDH is highly glycosylated relative to the flavin domain. The isoelectric point of the flavin domain is 5.45, that of the heme domain is 3.42 and that of CDH is 4.2 [21, 121]. CDH is thermostable and pH stable and it has maximum activity at room temperature for 24 h in a pH range of 3–10. CDH is highly stable between pH 3–5 and its stability decreases with an increase or decrease from this range. CDH has highest specificity for sugars mainly disaccharides and oligosaccharides and the k_{cat} (enzyme turnover number) for cellobiose reduction by CDH is ten times higher than glucose [21, 121]. Cellobiose is the most effective electron donor for CDH but many other reducing sugars can be used for electron transfer. CDH can reduce a wide range of electron acceptors, which include oxidative radicals, transition metals and two electron acceptors (quinones). Studies have reported that one electron acceptors are reduced preferentially at the heme domain [121]. CDH has a strong binding specificity for microcrystalline cellulose, once bound it cannot be easily eluted even at high pH, high salt concentrations, detergents or by cellobiose. It was reported that CDH inhibits LiP (lignin peroxidases) by reducing the veratryl alcohol and also can reduce compound II (intermediate formed during the catalytic cycle of LiP). CDH also reduces Mn^{3+} (redox mediator used by MnP) and also compound II of MnP similar to LiP [21, 121].

Mechanism CDH has the properties of a typical dehydrogenase with both oxidative and reductive reactions. CDH oxidizes the C1 position of a saccharide to a lactone which is spontaneously hydrolyzed to a carboxylic acid. The electrons taken up by the enzyme are later transferred to one or two electron acceptors [122, 123]**.** Substrate specificity of CDH is higher for cellobiose, cellodextrins, lactose, mannobiose and galactosylmannose. However, the later substrates have higher Km-values, the true substrates for CDH are di or oligosaccharides with reducing ends containing glucose or mannose residues. Monosaccharides such as glucose, mannose and maltose have very high Km values suggesting that there is binding of two glucose residues to the active site in separate subsites, at the same time monosaccharides have lower *Kcat* values then the di or oligo saccharides which suggests that binding of the β-dihexosides to the active site stimulates the catalysis creating an induced fit [124]. CDH also generates highly reactive hydroxyl radicals by a Fenton type reaction in the presence of an electron donor. Several studies were conducted to study the individual roles of the two prosthetic groups (flavin and heme domains) in the oxidation of compounds, which showed that oxidation of cellobiose (electron donor) is carried out by the FAD group which is further converted to $FADH_2$ and later transfers the electrons to the heme group (Fig. 4.7) [122, 123, 127]. Several groups have proposed a role for CDH in lignin depolymerization by reduc-

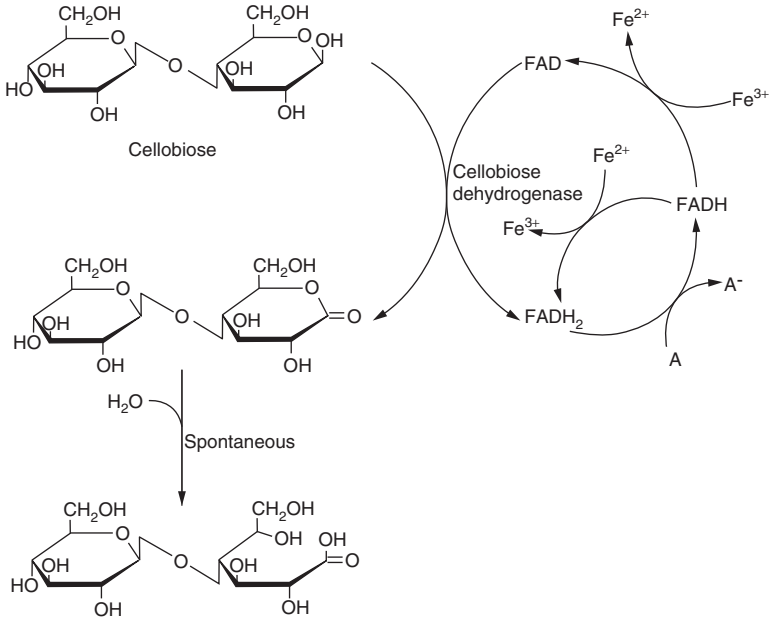

Fig. 4.7 Reactions of cellobiose dehydrogenase based on [125]. '*Fe*' represents the heme iron, '*A*' represents the one-electron acceptor (Reprinted with permission from Ref [126], Copyright ©2008, Oxford University Press)

ing phenoxy radicals thus preventing repolymerization of the radicals. Studies conducted by Henriksson et al. (1995) have showed that the CDH could stop the repolymerization of lignin model compounds, this was showed by incubating CDH with cellobiose, ferric ions, hydrogen peroxide and lignin model compounds. CDH generates highly reactive hydroxyl molecules that depolymerized the polymers showing that CDH does not depolymerize lignin or its subunits directly but hydroxyl radical groups are involved in the degradation of lignin related compounds [119, 128–130].

4.6 Lignin Degrading Auxiliary Enzymes (LDA)

Lignin degrading auxiliary enzymes are mostly H_2O_2 producers, as lignin degrading enzymes such as lacccase, LiP, MnP, VP require the presence of extracellular H_2O_2. Currently there are 7 enzymes classified as lignin degrading auxiliary enzymes (LDA): aryl alcohol oxidase (LDA1), vanillyl alcohol oxidase (LDA2), glyoxal oxidase (LDA3), pyranose oxidase (LDA4), galactose oxidase (LDA5), glucose oxidase (LDA6) and benzoquinone reductase (LDA7) (Fig. 4.8) [18]. Among these 7 different enzymes aryl alcohol oxidase, glyoxal oxidase are the most active hydrogen peroxide (H_2O_2) generating enzymes [120, 136].

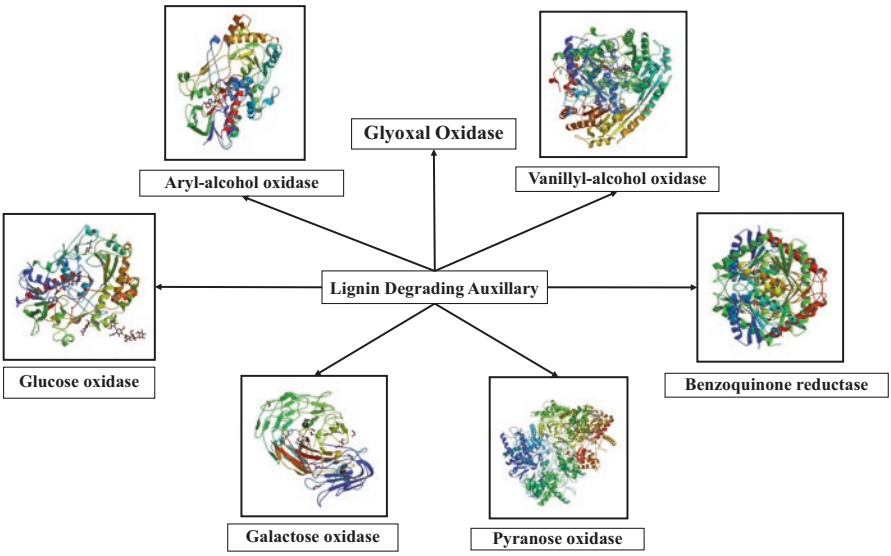

Fig. 4.8 Schematic representation of lignin degrading auxiliary enzymes namely, aryl alcohol oxidase (PDB ID: 3FIM) [131], vanillyl alcohol oxidase (PDB ID:1W1J) [132], glucose oxidase (PDB ID: 1CF3) [133], galactose oxidase (PDB ID: 2WQ8) [134], pyranose oxidase (PDB ID: 4MIF) [135]. benzoquinone reductase (PDB ID: 4LA4). All the above enzyme structures were obtained from PDB RCSB repository

4.6.1 Aryl Alcohol Oxidase

Aryl alcohol oxidase (AAO) (EC.1.1.3.7) was first observed in *Polystictus versicolor* or (*Trametes versicolor*) during the 1960s. Aryl alcohol oxidase was detected and characterized in white rot basidiomycetes such as *Pleurotus* species (*P. eryngii*), *Bjerkandera adusta* and a few ascomycetous fungi [137–141]. White rot fungi were found to be involved in efficient degradation of lignin, aryl alcohol oxidase was found to be involved in lignin depolymerization process by generating H_2O_2 and fueling ligninolytic peroxidases [137]. AAO is an FAD containing enzyme belonging to the glucose-methanol-choline oxidase (GMC) family of oxidoreductases. It was reported that AAO of Pleurotus eryngii was found to be involved in generation of peroxide by redox cycling of *p*-anisaldehyde (a fungal extracellular metabolite), in addition AAO also was found to be involved in oxidation of polyunsaturated primary alcohols [142]. Redox cycling of *p*-methoxylated benzylic metabolites by *P. eryngii* takes places through an oxygen activation reaction by AAO. Amino acid sequence comparisons of AAO revealed homology with glucose oxidase. AAO genes from *P. eryngii* and *Pleurotus pulmonarius* were cloned and sequenced [143]. For several years only the AAO sequence from *P.eryngii* was available, however recent advancements in genome sequencing and the sequencing of basidiomycetes genomes has revealed the sequence of around 40 AAO sequences and 112 GMC (glucose-methanol-choline oxidases) superfamily sequences were reported [144].

Kinetic isotope studies have showed that alcohol oxidation by AAO occurred by hydride transfer to the flavin domain and then hydroxyl proton transfer to the base [144]. At the same time site directed mutagenesis studies of AAO have showed that His502 is involved in activation of alcohol substrates by proton abstraction, this mechanism was later extended to other GMC oxidoreductases [144].

Structure Sequence comparison and structural analysis studies of AAO were conducted by Fernandez et al. (2009) and Varela et al. (2000). Aryl alcohol oxidase is a monomeric glycoflavoprotein with a molecular weight of 69.1 kDa with flavin adenine dinucleotide (FAD) as a cofactor. Primary structure analysis of AAO revealed that it belongs to the glucose-methanol-choline oxidoreductase family, the presence of consensus sequences such as N-terminal conserved βαβ dinucleotide binding motif (DBM) which are involved in FAD binding. According to Varela et al. (2000) AAO is composed of 593 amino acids of which 27 residues form a signal peptide, structural prediction analysis shows that it contains 13 putative α-helices and two major β-sheets where each major β-sheet contains six β-strands [145]. AAO showed 33 % sequence similarity with *Aspergillus niger* glucose oxidase and has a similar predicted secondary structure, at the same time it showed less homology with other oxidoreductases. The shape of AAO looks like an "elongated cylinder crowned by a cap, with dimensions of 75 Å 40 Å and 60 Å, respectively. Based on function, the protein can be divided into two domains: a substrate binding domain (cap region) and FAD binding domain (cylinder region). The FAD binding domain contains five stranded parallel β-sheets surrounding three α-helices and three stranded antiparallel β-sheets which is crosslinked to the other domains [131]. The additional crosslinked three stranded β-sheets are in return connected to another β-sheet motif of two antiparallel β-strands. The core substrate binding domain consisted of six stranded antiparallel β-sheets edged by two long α-helices (similar to the substrate binding domain of vanillyl alcohol oxidase) finally the central core of the substrate binding domain is covered by two pairs of two α-helices forming the widest portion of the cap [131]. The substrate binding domain and FAD binding domain are connected by three long nonstructured segments which spreads from one domain to the other domain, a second connection involves two extended two stranded parallel β-sheets which are present at the junction of the two domains [131]. The non-covalently bound FAD in AAO when compared to GO shows that the principle sites of FAD binding are on the ADP part of the molecule with βαβ protein interactions proving the role of flavin ring in substrate oxidation [146, 147]. Conserved amino acid residues between GO and AAO around the FAD group are G9, E33, G81, G86, S87, V231, A272, H502, D535, G536 and H546. Closer comparisons of the GO and AAO sequences show that the conserved amino acid residue N107 of GO involved in binding of the oxygen of ribityl moiety of FAD is replaced by H91 in AAO. At the same time the conserved amino acid residue E33 of AAO takes part in ADP-binding by hydrogen bonding with the O2' of ribose moiety [148].

Mechanism Structural and functional studies of AAO isolated from *P. eryngii* show that it has a variety of substrates, catalyzing the oxidation of primary and polyunsaturated alcohols [142]. The overall reaction mechanism of AAO can be

divided into an oxidative and a reductive reaction, first AAO catalyzes the oxidative dehydrogenation of the substrate (reductive reaction) later the flavin adenine dinucleotide is reoxidized by molecular oxygen, generating H_2O_2 (Fig. 4.9) [137]. Comprehensive studies of the substrate specificities of AAO revealed that it catalyses the oxidation of aromatic alcohols such as *p*-anisyl alcohol and aliphatic polyunsaturated primary alcohols to their corresponding aldehydes [142]. It was reported that phenolic hydroxyls strongly inhibits the enzymatic activity of AAO. The redox cycling of *p*-Anisaldehyde (important extracellular metabolite of *P. eryngii*) involves intracellular aryl-alcohol dehydrogenase along with AAO which results in hydrogen peroxide generation (Fig. 4.9) [149]. AAO seems to have a similar catalytic mechanism to choline oxidase (GMC oxidoreductase family) which catalyzes the oxidization of alcohol substrates resulting in the production of aldehydes. Earlier studies on AAO of *P. eryngii* shows that it catalyzes the conversion of primary alcohols of varied structural properties. AAO exhibits a wide range of electron donor substrate specificity by catalyzing the oxidation of aromatic and π-system containing primary alcohols such as benzylic alcohol, napthylic alcohol and aliphatic polyunsaturated alcohols [137, 142, 150]. The π-systems cause an increase in electron availability at the benzylic position causing hydride abstraction by the flavin N5 atom. The structural of the AAO active site prevents the oxidation of secondary alcohols as they cannot be accommodated at the appropriate distance from the catalytic histidine and flavin N5 atom due to the presence of Phe501 [151]. Bisubstrate kinetic analysis with different benzylic alcohols shows the overall AAO catalytic cycle is highly influenced by the nature of substituents on the benzene ring. AAO catalysis is divided into a reductive and oxidative reactions, when it is treated with electron

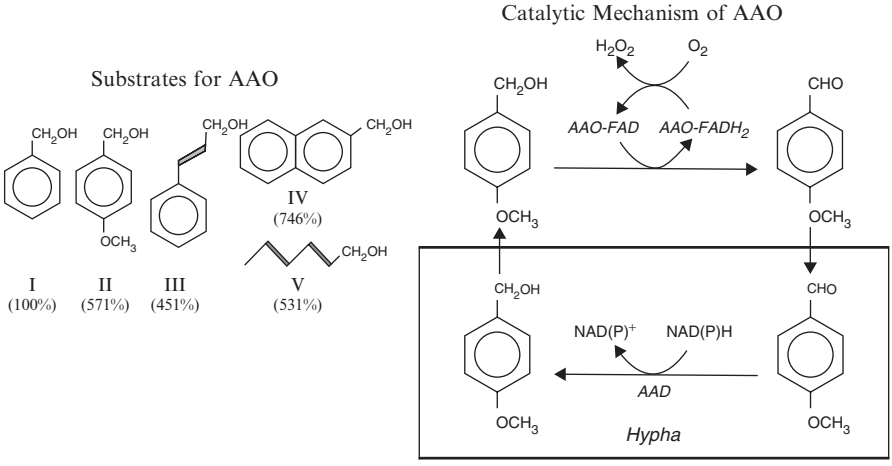

Fig. 4.9 Chemical structure of various substrates of *Pleurotus* AAO (I, benzyl alcohol; II, p-anisyl alcohol; III, cinnamyl alcohol; IV, 2-naphthalenemethanol; and V, 2,4-hexadien-1-ol) and relative activity estimated as O_2 consumption [142]. Scheme for H_2O_2 production by anisaldehyde redox-cycling involving extracellular AAO and intracellular AAD (Reprinted with permission from Ref [145], Copyright © 2000, Elsevier)

withdrawing substrates such as 3-chloro and 3-fluorobenzyl alcohols both t half reactions become independent resulting in aldehyde product dissociation before the oxygen reaction by a ping-pong steady state mechanism [152]. In electron donor substituents such as methoxylated benzyl alcohols, oxygen reacts with the reduced AAO-aldehyde complex resulting in a ternary complex prior to aldehyde product release [152]. The catalytic cycle of AAO depends on the stacking and stabilizing interactions of aromatic substrate and product at the active site Tyr92 residue (involved in stabilization of alcohol substrate) which occur by switching between ternary and ping-pong mechanisms [152].

4.6.2 Vanillyl Alcohol Oxidase

Vanillyl alcohol oxidase (EC.1.1.3.38) is a flavin containing protein which was first isolated from *Penicillium simplicissimum* based on its ability to oxidize vanillyl alcohol to vanillin, 4(methoxymethyl) phenol to 4-hydroxybenzaldehyde [153]. It was also studied for its ability to degrade lignin. Vanillyl alcohol oxidase (VAO) can convert phenolic compounds by different catalytic processes such as oxidation, deamination, demethylation, hydroxylation and dehydrogenation [154]. The reaction mechanism of VAO for oxidation of 4(methoxy methyl) phenol involves a primary transfer of hydride from the substrate to the flavin leading to the formation of a two electron reduced enzyme complex with a *p*-quinone methide compound as an intermediate. Further the reduced flavin is reoxidized by oxygen associated with hydration of *p*-quinone methide [155] VAO is an industrially important enzyme for the production of the compounds: vanillin, 4-hydroxybenzaldehyde, coniferyl alcohol and pure phenolic derivatives [154].

Structure Crystallographic studies of VAO were first reported by Mattevi et al. (1997). The VAO protein structure consists of 560 amino acid residues with a covalently bound FAD cofactor. VAO has two major subunits: a larger domain (FAD-binding domain, smaller cap domain (FAD isoalloxazine ring). The larger FAD-binding site consists of amino acids ranging between 6–270 and 500–560 which form one antiparallel sheet with six α-helices surrounding one mixed β-sheet [154, 156]. Smaller domain (FAD-isoalloxazine ring) consists of amino acids271–499 constituting large seven stranded antiparallel β-sheets bordered on both sides by seven α-helical regions. The structure of VAO resembles that of PCMH (both enzymes are FAD-dependent oxidoreductases) with an rms deviation of 1.2 Å for about 470 Cα atom pairs showing about 31 % of amino acid sequence similarity. In solution, vanillyl alcohol oxidase is an octamer of eight identical subunits. The crystal packing of VAO reveals an oligomer with tetragonal crystals[157]. The VAO octamer has 42 symmetry with a fourfold axis and a similar crystallographic axis The oligomer consists of tetramers of dimers and each dimer is stabilized by extensive intersubunit contacts, burying 18 % of the monomer surface area upon dimer formation [154]. However, upon octamer formation only 5 % of the monomer surface area is buried [156]. The flavin ring in VAO is covalently bound to His-422 and

the flavin is planar, not distorted by the covalent attachment. The crystal structures of four VAO ligand complexes reveal the remarkable architecture of the VAO active site, comprising an elongated cavity which is not accessible by solvent. Amino acid residues Tyr108, Tyr503 and Arg 504 form an anion binding site (activates the substrates by stabilization of its phenolate form),. The binding of ligands within the catalytic cavity is well matched with substrate oxidation, commencing via direct hydride transfer from Cα atom to the N5 atom of flavin domain [154, 156, 157]. Earlier structural studies showed that Asp-170, situated near the N5 atom of the flavin was an active site base. Site directed mutagenesis conducted by Van den Heuvel et al. (2000) reported on the catalytic role of Asp-170 in VAO. It was showed that active site amino acid residue Asp-170 is involved in catalysis and covalent flavinylation [153]. Van den Heuvel et al. (2000) carried out kinetic characterization studies of VAO variants and reported that Asp-170 mutants are 50 % less active than the wild type enzyme. The Asp-170 variants also showed that the reduced catalysis was due to the flavin reduction. Mutant proteins lost the ability to form a stable complex between the reduced enzyme and a *p*-quinone methide intermediate. Thus, supporting the role of Asp-170 in the process of autocatalytic flavinylation and efficient redox catalysis [153]. A structural study conducted by van den Heuvel et al. (2000), showed changing the stereospecificity of the active site by relocating an active site amino acid to the opposite side by site directed mutagenesis effected the catalysis of VAO [158]. This study confirms the role of Asp-170 in VAO for efficient redox catalysis and also the stereospecificity of VAO, showing that VAO is highly stereospecific for the production of alcohols [158].

Mechanism Based on spectroscopic and kinetic studies it was shown that substrate oxidation commences via direct hydride transfer from the Cα atom to N5 of flavin adenine dinucleotide. As a result a *p*-quinone methide (intermediate) is formed which is further activated by the preferential binding of the phenolate form of the substrate, this is supported by the three dimensional structure of the VAO [156]. Studies of VAO binding with VAO-isoeugenol, VAO-2-nitro-*p*-cresol complexes shows that VAO achieves hydride transfer from the Cα atom 3.5 Å from N5 atom. The hydroxyl oxygen is bound to three residues: Arg504, Tyr503 and Tyr108 through hydrogen bonds which stabilize the negative charge of the phenolate ion [156]. Under anaerobic conditions, VAO reaction with 4-methoxymethyl phenol results in a stable reduced enzyme-*p*-quinone methide complex, however the final product is synthesized and released immediately after exposure to oxygen, following FAD reoxidation. From three dimensional structures of VAO, it is suggested that charge stabilizations between the flavin, quinone intermediate and Arg-504 regulate the catalytic cycle. Besides its role in interacting with the phenolate oxygen, Arg-504 is involved in balancing the negative charge on the N1-C2=O2 locus of the anionic reduced cofactor. The C2 atom of flavin deviates from its expected position due to the oxygen atom of *p*-quinonemethide molecule binding to the reduced enzyme [156]. Thus in the reduced enzyme, the negative charge of the flavin C2 atom causes electrostatic repulsion which prevents the formation of a phenolate ion resulting in the stabilization of the quinone intermediate form. Upon reoxidation of

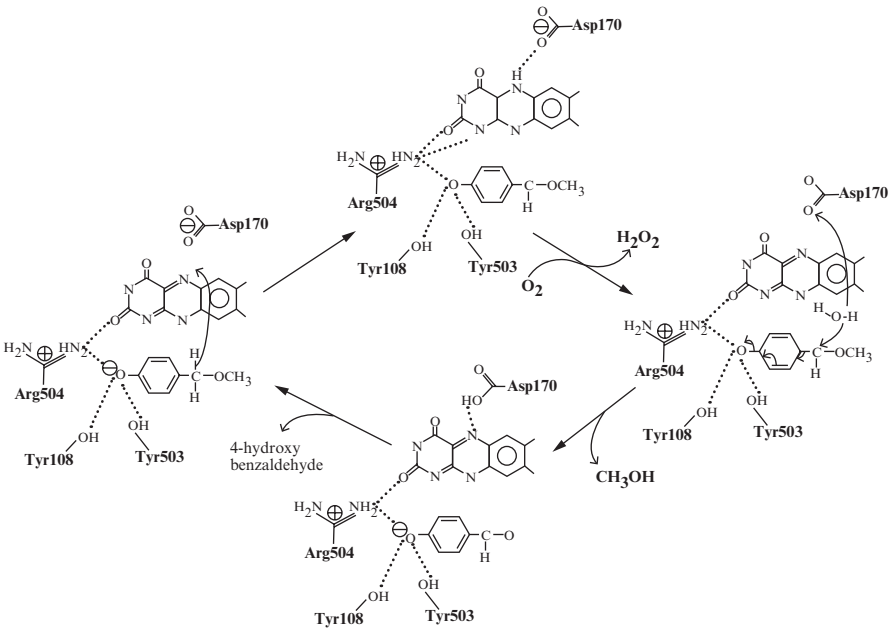

Fig. 4.10 The reaction mechanism for the oxidation of 4-(methoxymethyl) phenol. In the first step, the substrate is oxidised via a direct hydride transfer from the substrate Cα atom to the N5 of flavin. The reduced cofactor is then reoxidised by molecular oxygen with the production of a hydrogen peroxide molecule. In the next step, the p-quinone-methoxymethide intermediate is hydroxylated by a water molecule, possibly activated by Asp170. The resulting 4-hydroxybenzaldehyde and methanol products are released (Reprinted with permission from Ref [156], Copyright © 1997, Elsevier)

flavin, Arg-504 lacks an anionic partner which triggers the development of negative charge on the oxygen atom of the quinone group. The electrophilicity of the methide carbon is increased enabling hydroxylation of 4-methoxymethyl phenol or deprotonation of the intermediate (vanillyl-alcohol) thus generating the final product (Fig. 4.10) [156, 157].

4.6.3 Glyoxal Oxidase

Glyoxal oxidase an extracellular hydrogen peroxide producing enzyme secreted by lignolytic cultures of *P. chrysosporium* [159]. Glyoxal oxidases catalyzes the oxidation of wide range of aldehydes and α-hydroxyl carbonyl compounds by reducing O_2 to H_2O_2, thus glyoxal oxidase fuels the process of lignin degradation by generating H_2O_2 which is used by ligninolytic peroxidases (such as lignin peroxidase, manganese peroxidase) [159, 160]. Glyoxal (OHCCHO) and methylglyoxal (CH_3COCHO) are two well known substrates for glyoxal oxidase in the extracellular fluids of lignolytic cultures [161].

Structure Glyoxal oxidase was isolated and characterized from the supernatants of lignolytic cultures of *P. chrysosporium*. Little was known about the structure and function of glyoxal oxidase until recently.. Studies have shown that glyoxal oxidase is a monomeric acidic glycoprotein with a molecular mass of 57 kDa [161]. It is a copper metalloenzyme with a free radical coupled copper active site similar to that of galactose oxidase. Both glyoxal oxidase and galactose oxidase have a conserved mononuclear copper radical active site coordinated by two histidine residues (His-496–His581) and two tyrosine residues, one unmodified (Tyr-495) and the covalently modified tyrosine (Tyr272), which is crosslinked to (Cys-228) thus forming a new dimeric (cysteine-tyrosine) bond. Sequence comparison of glyoxal and galactose oxidase show they have a homology of only 20 % [162, 163]. Spectrographic studies have shown a remarkable degree of similarity between them at their active site, both in structure and chemistry. These studies suggested that glyoxal oxidase and galactose oxidase are functional variants catalyzing distinct reactions at their identical active sites [159]. Glyoxal oxidase has a broad pH optimum with maximum enzyme activity at pH6. A wide range of simple aldehydes, α-hydroxycarbonyl and α-dicarbonyl compounds were found to act as substrates however highest activity was observed with methylglyoxal and it has no activity on glucose, xylose, cellobiose, galactose or other sugars [161].

Mechanism Studies have revealed that *P. chrysosporium* secretes three extracellular enzymes: lignin peroxidase, manganese peroxidase and glyoxal oxidase. Glyoxal oxidase fuels the complete ligninolytic mechanism by generating extracellular H_2O_2, which is required for the functioning of lignolytic peroxidases [164]. Pure glyoxal oxidase is inactive, however it is activated by peroxidases and peroxidase substrates) [164]. Though glyoxal and methylglyoxal (substrates) of glyoxal oxidase were observed in ligninolytic cultures, there are other substrates such as formaldehyde, acetaldehyde, glycolaldehyde, glyoxylic acid, dihydroxyacetone, glyceraldehyde. In addition, downstream lignin degradation products act as substrates for glyoxal oxidase [164]. Glyoxal oxidase has an efficient sequential oxidation process by converting glycolaldehyde to oxalate (glycolaldehyde → glyoxal → glyoxalate → oxalate) The catalytic mechanism behind oxidation of aldehydes by glyoxal oxidase is not known, however it was suggested that it oxidizes substrates similarly to galactose oxidase.

4.6.4 Pyranose Oxidase

Pyranose oxidase (EC.1.1.3.10; oxygen 2-oxidoreductase) is a hydrogen peroxide producing enzyme. Pyranose oxidase catalyzes the oxidation of the C-2 of several aldopyranoses, D-glucose is a ideal substrate for the enzyme [165–167]. Several fungi belonging to basidiomycetes and particularly members of the order *Aphyllophorales* secrete extracellular pyranose oxidase[168]. The structure and catalytic mechanism of pyranose oxidase were extensively studied in *Trametes*

multicolor fungi,. Its amino acid sequence suggests that it belongs to the glucose-methanol-choline (GMC) family of flavin adenine dinucleotide (FAD) dependent oxidoreductases [169]. Pyranose oxidase is a large flavoproteins which can oxidize a number of monosaccharides at their carbon-2 position in the presence of molecular oxygen, producing 2-keto sugars and hydrogen peroxide [168].

Structure Structural studies of pyranose oxidase protein were carried out by Hallberg, BM et al. (2004). Pyranose oxidase is a homotetramer localized in the hyphal periplasmic space of ligninolytic cultures of fungi with a molecular mass of 270 kDa [170]. Its amino acid sequence and protein structure show that it belongs to the glucose-methanol-choline (GMC) family of long chain oxidoreductases with a large FAD domain. Its structure consists of a six stranded central β-sheet and three α-helices [170]. The large homodimer contains a large internal cavity of 15,000 Å, which has four active sites [170]. Pyranose oxidase from *Trametes multicolor* is a homotetramer and its cavity serves as a storage site for quinones generated during lignin degradation [170]. The cavity prevents diffusal of toxic quinines until they are reduced by pyranose oxidase. The enzyme oxidizes polymeric carbohydrates substrates, when compared to other FAD-dependent enzymes such as GMC-enzymes. The FAD is linked covalently by its α-methyl group to the N^{e2} atom of His-167 [170]. The active sit of the enzyme retains the typical amino acid residues of catalytic GMC-type enzymes such as a His-Asn pair below the isoallaxazine ring of the FAD domain [170]. Docking studies of D-glucose in the pyranose oxidase active site suggests that the active site loop under goes dynamic changes during the reductive half reaction allowing the binding of carbohydrates [170]. These studies also suggest that the active site loop is involved in the regioselective catalysis of aldopyranoses at their C2 and C3 positions by pyranose oxidase [170].

Mechanism Pyranose oxidase is an hydrogen peroxide generating enzyme which catalyzes the oxidation of D-glucose and other aldopyranoses at the C-2 position resulting in the production of 2-keto sugars it was also found to be involved in lignin depolymerization. It catalyses the regioselective oxidation of different aldopyranoses at their C-2 position using molecular oxygen resulting in 2-keto aldoses and H_2O_2. The whole reaction can be divided into an oxidative and a reductive reaction, in the reductive half reaction the sugar is oxidized to a keto sugar followed by reduction of FAD. The oxidative reaction involves the reduction of O_2 to H_2O_2 and reoxidization of the FAD [168, 171]. Pyranose oxidase also oxidizes certain compounds at the C-3 position such as 2-deoxy-D-glucose, 2-keto-D-glucose and methyl-β-D-glucosides [172, 173]. The (k_{cat}/K_m) is highest for β-D-glucose. Studies have reported that pyranose oxidase also oxidizes monosaccharides such as D-xylose, D-galactose and L-arabinose (constituents of hemicellulose) with lower catalytic efficiencies, which may extend the enzymes ability to generate hydrogen peroxide from the lignincellulose derived sugars. The optimum pH of the enzyme varies based on the type of electron acceptors used ie oxygen, various quinones and radicals. Quinones and radicals are the best substrates of pyranose oxidase, suggesting its role in lignin depolymerization is as a hydrogen peroxide generating and

quinone reducing enzyme. It was reported that pyranose oxidase from *Phlebiopsis gigantea* has the ability to hydrolyze β 1 → 4 linked disaccharides (cellobiose and lactose) and α 1 → 4 linked disaccharides (such as maltose) to the corresponding monosaccharides at their C2 position [174]. β glycosides of higher alcohols such as hexyl, phenyl, o-nitrophenyl and p-nitrophenyl) are converted to disaccharides by pyranose oxidase through a glycosyl transferase reaction [174].

4.6.5 Galactose Oxidase

Galactose oxidase (EC 1.1.3.9) an extracellular enzyme secreted by *Fusarium spp.* Galactose oxidase is a monomeric enzyme containing a single copper ion, catalyzing the oxidation of primary alcohol substrates (D-isomers) such as D-galactose and other polysaccharides containing D-galactose on their reducing ends resulting in the production of aldehydes and hydrogen peroxide [175, 176]. Galactose oxidase belongs to the alcohol oxidoreductase family (also known as alcohol oxidase), enzymes belonging to this generally use molecular oxygen as electron acceptors for generating hydrogen peroxide [177]. Most alcohol oxidoreductases are flavoproteins that use FAD+ as primary electron acceptors, however some of these enzymes are copper radical containing oxidases (CROs) such as galactose oxidase, glyoxal oxidase and hexose-1-oxidase [177].

Structure The structure and catalytic mechanism of galactose oxidase were extensively studied by biochemical and spectroscopic methods. Galactose oxidase has a mass of 68 kDa consisting of three major β structure domains and single α-helix (amino acid residues 327–332) [178]. The presence of three β structures in the protein imparts structural stability, The first domain has a β sandwich structure (amino acid residues 1–155) that is linked to the second domain by polypeptide chains. The second domain is the largest domain residues 156–532, it has pseudo sevenfold symmetry. The third domain (residues 533–639) is on the opposite side of the second domain from the copper [178]. The structure of galactose oxidase is similar to that of glyoxal oxidase, containing a mononuclear copper radical with a crosslinked cysteine-tyrosine residue along with one unmodified axial tyrosine and a histidine side chain as coordinating residues [177]. The active site of the galactose oxidase contains a copper complex with two tyrosine (Tyr 272 and Tyr495) and two histidine (His496 and His581) amino acid side chains [178]. One of the tyrosine residue (Tyr272) was found to be crystallographically crosslinked to the carbon atom (Cε) of a phenolic side chain and the sulfur (Sγ) of Cys228, forming a thioether Tyr-Cys bond. The thioether bond formed between Tyr-Cys affects both the structure and function of the protein, structurally this crosslinking also affects the active site by making it more rigid similar to a disulfide bond [178].

Mechanism Galactose oxidizes primary alcohols resulting in the production of aldehydes and hydrogen peroxide. This is a two electron reaction with only one copper ion at the active site and a second redox active center, a tyrosine residue. Tyr-272 also acts as ligand to the copper ion [178]. The catalytic mechanism of galactose

oxidase can be divided into two reactions (a) proton transfer from the O-6 position of galactose to the axial tyrosine anion (hydrogen atom transfer) then from the C6 of galactose to the Tyr-Cys radical cofactor followed by electron transfer from the carbohydrate, generating an aldehyde and Cu^{+} [177]. In the second half of the reaction electron transfer continues from Cu+ to oxygen by producing superoxide then through hydrogen transfer, a proton is transferred from the phenolic hydroxyl group of the Tyr-Cys cofactor to superoxide, producing a metal bound hydroperoxide. The final proton transfer from the axial tyrosine to hydroperoxide generates hydrogen peroxide and Cu^{2+} (resting state of the enzyme) [177].

4.6.6 Glucose Oxidase

Glucose oxidase (E.C.1.1.3.4) is an important H_2O_2 generating oxidoreductase produced by ligninolytic cultures of *P. chrysosporium*. Glucose oxidase catalyzes the oxidation of β-D-glucose to gluconic acid, using molecular oxygen (as electron acceptor) thus producing H_2O_2 [179, 180]. Glucose oxidase has several commercial applications such as increasing the quality of food materials (color, flavor and shelf life), oxygen removal from fruit juices and canned food etc [180]. Apart from these applications, glucose oxidase also inhibits different food-borne pathogens such as *Salmonella infantis, Staphylococcus aureus, Clostridium perfringens, Bacillus cereus, Campylobacter jejuni* and *Listeria monocytogens* [181].

Structure Glucose oxidase (GOD) is a homodimeric glycoprotein containing two identical polypeptide chains that are covalently linked together by disulfide bonds. The molecular mass of glucose oxidase ranges from 130 to 175 kDa [182], containing two molecules of FAD which bind tightly to the protein thus maintaining its three dimensional structure. The structure of glucose oxidase from *P. amagasakiense* shows that each of the protein subunit contains one mole of tightly bound FAD. GOD has a very high specificity for β-D-glucose as α-D-glucose is not a suitable substrate for GOD. Very low activity was observed when 2-deoxy –D-glucose, D-Mannose or D-Galactose were used as substrates. Metals such as Ag+, Hg 2+, Cu2+ and chemicals such as hydroxylamine, hydrazine, *p*-chloromercuribenzoate, phenylhydrazine, dimedone and sodium bisulphate inhibit the activity of GOD [183, 184]. GOD from *P. amagasakiense* was found to be glycosylated predominantly with mannose residues, with a total carbohydrated content of 11–13 % [183, 184]. Structural studies of GOD from *A. niger* and *P. amagasakiense* were found to contain similar carbohydrate residues such as glucose, mannose and hexosamine. *A. niger* GOD showed higher mannose and hexosamine and less glucose then *P. amagasakiense* GOD, resulting in total carbohydrate contents of 16 % (*A. niger*) and 11 % (*P. amagasakiense)* respectively. The active site of *P. amagasakiense* GOD contains: Tyr-73, Phe-418, Trp-430, Arg-516, Asn-518, His-520 and His-563. Arg-516 and Asn-518 (lesser extent) were found to be required for the efficient binding of β-D-glucose by GOD [185]. Aromatic amino acids such as Tyr-73, Phe-418 and Trp-430 were required for the correct orientation of the substrate and also for speeding up the

oxidation of glucose molecules. His-520 and His-563 are involved in hydrogen bond formation to the hydroxyl group (1-OH) of glucose during the reaction. *A. niger* GOD contained more histidine, arginine, tyrosine and less lysine, phenylalanine then *P. amagasakiense* GOD [184, 185].

Mechanism The reaction of GOD can be divided into an oxidative step and a reductive step. The reductive step of GOD oxidizes β-D-glucose to D-glucano-δ-lactone which is further hydrolyzed to gluconic acid (non-enzymatically). In *A. niger* a lactonase catalyzes the hydrolysis of D-glucano-δ-lactone to gluconic acid. It also reduces the FAD domain of GOD to $FADH_2$ [185]. Reduced GOD is re-oxidized by molecular oxygen to H_2O_2 in the oxidative reaction, H_2O_2 from the above reaction is cleaved by catalase producing water and oxygen [186]. The flavin domains of GOD are involved in the redox reaction, during the oxidative reaction of GOD and electrons from electron donors are transferred to the isoalloxazine nucleus of flavin domain (FMN) and then to the electron acceptor [187]. GOD catalyzes the reaction by transferring the electrons from glucose to oxygen, producing H_2O_2, thus placing GOD in the oxidoreductase class of enzymes. Overall enzyme catalysis of GOD depends on oxidation and reduction reaction steps of its flavin group (FAD) primarily glucose reduces the FAD to $FADH_2$ by producing gluconic acid (product) without forming free radical containing semiquinone (intermediate). At the same molecular oxygen (electron acceptor) reduces the $FADH_2$ back to FAD generating H_2O_2 as a product (Fig. 4.11) [187].

4.6.7 Benzoquinone Reductase

The 1,4-Benzoquinone reductase (EC.1.6.5.6) is an intracellular enzyme which was purified and characterized from the agitated cultures of *P. chrysosporium*. 1,4-Benzoquinone reductase was expressed in both nitrogen sufficient and limited conditions [188, 189]. *P. chrysosporium*, one of the highly studied lignin degrading

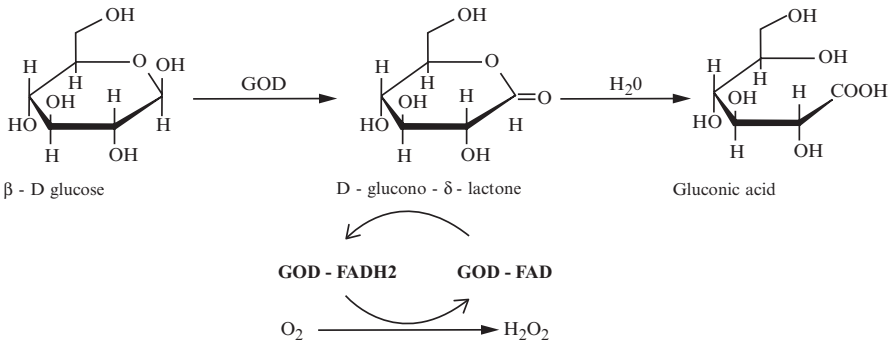

Fig. 4.11 Reaction mechanism of glucose oxidase (GOD) [185] (Reprinted with permission from Ref [179], Copyright © 2009, Elsevier)

fungi, secretes two classes of ligninolytic peroxides: lignin peroxidase(LiP)and manganese peroxidase(MnP) along with several H_2O_2 generating enzymes. These enzymes catalyze the primary steps of lignin depolymerization resulting in a wide variety of intermediate products such as substituted quinones, hydroquinones, benzaldehydes and other ring opened fragments. Methoxylated lignin derived quinones are reduced by intracellular quinone reductases [188, 189].

Structure The 1,4-Benzoquinone reductases from *P. chrysosporium* was purified and characterized. These studies showed that it is a NADPH dependent 1,4-benzoquinone reductase with a molecular mass of 44 kDa containing two similar 22 kDa subunits which contain flavin mononucleotide [189]. Purified 1,4-benzoquinone reductase shows a typical oxidized flavin spectrum from 375 to 450 nm [188]. Upon reduction of the enzyme with sodium dithionate a drop in absorbance of the flavin was observed. The presence of flavin was proved by two methods, the released flavin from the boiled enzyme was isolated using ultrafiltration., HPLC analysis of the ultrafiltrate had same retention time as standard flavin mononucleotide (FMN), secondly fluorescence of the flavin isolated from the enzyme showed a pH dependence identical to FMN [188, 189]. Purified quinone reductase uses either NADH or NADPH as its electron donor with Km for NADH (55 μM) and NADPH (48 μM) respectively. 2-MBQ and 2-DMBQ were two substituted paraquinones identified as fungal metabolites of lignin model compounds, quinone reductases are capable of reducing both paraquinones and ortho quinones. 2-DMBQ is one of the best substrate for quinone reductases because of its stability and being a downstream product produced during oxidation of lignin model compounds. Quinone reductase showed a high turnover for 2-MBQ and 2-DMBQ which suggests a role for this enzyme in the degradation of lignin and related compounds [188, 189].

Mechanism Benzoquinone or quinone reductases are significant enzymes secreted by several fungi especially *P. chrysosporium.* 1,4-Benzoquinone reductase is a NADPH dependent intracellular enzyme, it contains flavin mononucleotide (FMN). 1,4-Benzoquinone reductase was active during both primary and secondary metabolism but the enzyme inducers are stronger during the primary metabolic processes [188–190]. Studies showed that when vanillate or methoxy-*p*-quinone are added to cells, carrying out primary metabolism, enzyme expression was increased. However, the effect was small when the same compounds were added to secondary metabolic cells, which suggests that quinone reductase is regulated independently of lignin and manganese peroxidase [188]. LiP and MnP are expressed only during the secondary metabolic stage of the growth and the there expression is not induced by aromatic substrates. The regulation of quinone reductases is similar to that of vanillate hydroxylase, which suggests its involvement in vanillate metabolism [188–190]. Quinone reductase was expressed during the lignolytic phase of *P. chrysosporium*, suggesting a role in the reduction of quinones generated during lignin degradation. It was reported that quinone reductases are induced upon quinone addition, suggesting the involvement of quinone reductase in lignin and quinone degradation [188–190]. Besides degrading of quinone and lignin derived compounds, it is also reported that quinone reductases protects *P. chrysosporium*

from oxidative stress by acting as redox active toxins. Quinones obtained by metabolic conversion are reduced by one electron generating semiquinone radicals, which are then oxidized by oxygen generated super oxide anion, this superoxide anion is further converted to H_2O_2 through superoxide dismutase and later in the presence of suitable electron donors it results in production of highly reactive hydroxyl radicals from H_2O_2 [188–190]. The detailed mechanisms of the regulation and catalytic mechanism of quinone reductase need to be explored (Table 4.3).

4.7 A Short Note on Genome Sequencing Studies of Lignin Degrading Fungi

In 2004, Martinez et al., had sequenced the whole genome sequence of *Phanerochaete chrysosporium* [206]. As it was the first wood decaying fungus to be sequenced from the phylum Basidiomycota there were few difficulties in annotating the whole genome. In the year 2006, Vanden Wymelenberg et al. have improved the genome assembly and reannotated the *P. chrysosporium* genome [207]. *P. chrysosporium* genome has revealed a wide array of hydrolytic and oxidative enzymes mainly class-II peroxidases apparently supporting its lignocellulose degrading ability. Later in the year 2009, complete genome sequencing of *Postia placenta* was performed by Martinez et al, genome of *P. placenta* has revealed several interesting facts about its wood decaying patterns. *P. placenta* genome lacks genes coding for peroxidases, few genes coding for enzymes involved in degradation of crystalline cellulose (GH6, GH7 and GH61) [208]. However, these studies have reported that *P. placenta* genome codes for enzymes involved in generating Fenton reagents (reactive oxygen species). Whole genome sequences of prominent brown rot fungus such as *Serpula lacrymans* [209], *Fibroporia radiculosa* [210] have shown similar results such as lacking the genes coding for peroxidases, reduced expression of genes coding for CAZymes and possessing oxidoreductases involved in Fenton reactions. The genome sequence of the *Schizophyllum commune* was first wood decaying fungus to be sequenced from order Agaricales [211]. Though it was reported to degrade lignin, *S. commune* lacked the genes coding for peroxidases. While whole genome sequencing of several white rot fungus such as *Ceriporiopsis subvermispora* [212], *Phanerochaete carnosa* [213], *Heterobasidion irregulare* [214], *Laccaria bicolor* [215], *Volvariella volvacea* [216], *Agaricus bisporus* [217], *Armillaria mellea* [218] etc., have revealed several significant facts about lignocellulose degrading enzymes and their corresponding mechanisms [219]. Large scale genome comparison studies showed that whiterot fungi has wide range of genes coding for lignocellulolytic enzymes compared to brown rot fungi [220]. Especially enzymes involved in breakdown of crystalline cellulose such as GH6, GH7, GH61 and CBM1 are predominant in white rot fungi. Similarly whiterot fungi possess several genes coding for peroxidases, whereas in most of the brown rot fungi genes coding for peroxidases are mostly absent or reduced [220, 221].

These sequencing studies has dramatically raised the interest in sequencing projects of wood decaying fungi. The large scale sequencing projects like 1000 Fungal Genome Project, Joint Genome Institute (JGI) are playing a critical role in revealing

Table 4.3 Catalytic mechanisms and structural studies of different lignin degrading auxiliary enzymes (LDA)

Enzyme and FOLy class	Catalytic mechanism	Structural studies and reference
Aryl alcohol oxidase (LDA1) EC 1.1.3.7	$\text{Aromatic primary alcohol} + O_2 \rightarrow \text{Aromatic aldehyde} + H_2O_2$	*Pleurotus eryngii* [131, 191–193]
Vanillyl alcohol oxidase (LDA2) EC 1.1.3.38	$\text{Vanillyl alcohol} + O_2 \rightarrow \text{vanillin} + H_2O_2$	*Penicillium simplicissimum* [153, 156, 158, 194, 195]
Glyoxal oxidase (LDA3) EC 1.1.3.-.	Glyoxal oxidase catalyzes oxidation of wide range of simple aldehydes, α-hydroxy carbonyl compounds by producing hydrogen peroxide	*Aspergillus nidulans, Pichia pastoris, Phanerochaete chrysosporium* [160, 196, 197]
Pyranose oxidase (LDA4) EC 1.1.3.10	$FAD_{(Oxidized)} + D\ \ Glucose \rightarrow FAD_{(Reduced)} + 2\ \ keto\ \ D\ \ glucose$ $FAD_{(Oxidized)} + O_2 \rightarrow FAD_{(Reduced)} + H_2O_2$	*Trametes multicolor* [170, 198–200], *Peniophora* sp. [201, 202] *Phanerochaete chrysosporium* [135]
Galactose oxidase (LDA5) EC 1.1.3.9	$D\ \ \text{Galactose} + O_2 \rightarrow D\ \ \text{Galacto}\ \ \text{hexodialdose} + H_2O_2$	*Aspergillus nidulans, Pichia pastoris* [175–178, 203, 204]
Glucose oxidase (LDA6) EC 1.1.3.4	$\beta\ \ D\ \ \text{glucose} + O_2 \rightarrow D\ \ \text{glucono}\ \ 1,5\ \ \text{lactone} + H_2O_2$	*Aspergillus niger* [146, 205]
Benzoquinone reductase (LDA7) EC 1.6.5.6	$NADPH + H^+ + p\ \ \text{benzoquinone} \rightarrow NADP^+ + \text{hydroquinone}$	*Phanerochaete chrysosporium* [188–190]

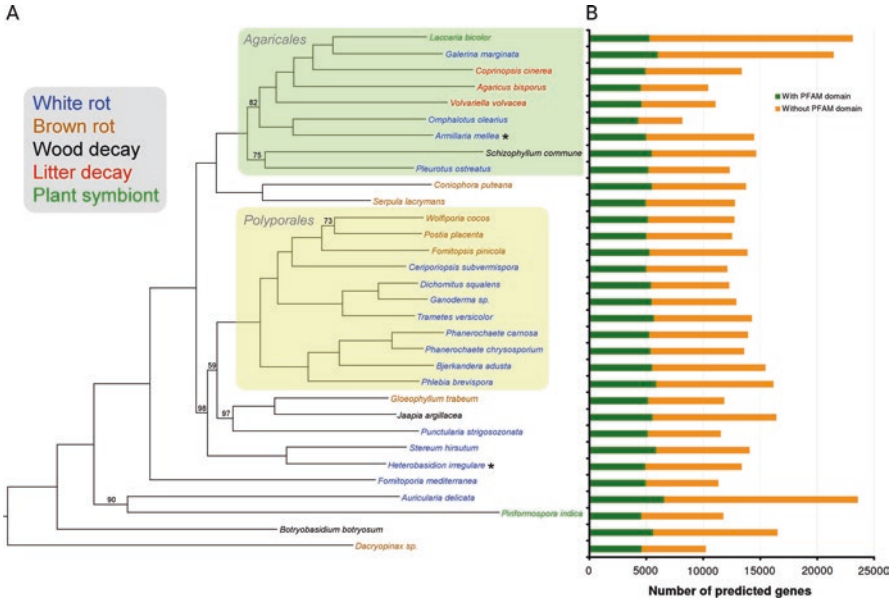

Fig. 4.12 (**a**) Phylogeny and main lifestyles of Agaricomycetes with a published genome sequence. The major orders Agaricales and Polyporales are indicated. The majority of these species are wood decayers and can be further classified as either white rot fungi (which degrade all components of the plant cell wall) or brown rot fungi (which modify lignin, but do not break it down to a large extent). *Schizophyllum commune*, *Jaapia argillacea* and *Botryobasidium botryosum* are also wood decayers, but cannot be easily classified as either white or brown rot fungi. *Coprinopsis cinerea*, *Agaricus bisporus* and *Volvariella volvacea* are saprotrophs growing on non-woody substrates. The ectomycorrhizal fungus Laccaria bicolor and the endophyte Piriformospora indica both form interactions with plant roots. Species with an asterisk (*) are predominantly plant pathogens. The genomes of *G. marginata*, *P. ostreatus*, *J. argillacea* and *B. botryosum* have been submitted for publication. (**b**) Number of predicted genes for each genome. Each bar lines up with a species from the tree in (**a**). The total number of genes varies per genome, but the number of genes with at least one PFAM domain is more constant. Genes without a PFAM domain outnumber those with a PFAM domain, showing that much remains to be learned about these organisms (Reprinted with performance from Ref [219], Copyright © 2014 Elsevier)

and understanding the whole genome of sequences of several fungi (Figs. 4.12 and 4.13). The JGI have also developed a strong web based interactive and integrated genome analysis portal called MycoCosm [222]. As of 2016 JGI MycoCosm offers over 563 sequenced and annotated fungal whole genome sequences. As most of the wood decaying fungi were reported from the phylum Basidiomycota out of which 202 fungal genome sequences belongs to the phylum Basidiomycota. Among Basidiomycetes fungi 159 fungal genome sequences reported belongs to subphylum Agaricomycotina, 16 and 27 fungal genome sequences belong to Ustilaginomycotina and Pucciniomycotina respectively. Thus, the recent advancements in genomics field in the past decade has prominently improved our understanding the genes involved in coding for the lignocellulose degrading enzymes and their pathways [219].

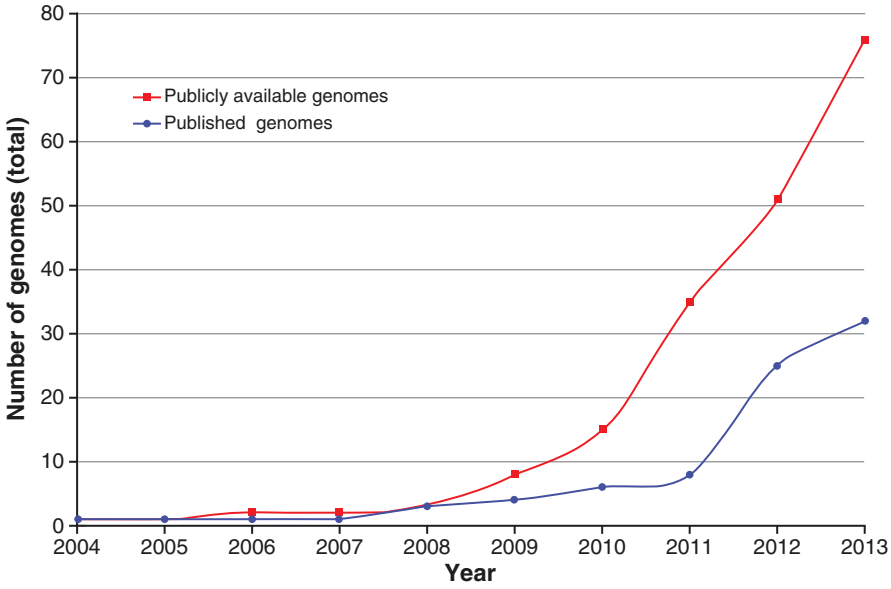

Fig. 4.13 The number of available genome sequences of the Agaricomycetes has dramatically increased over the past decade. For each year, the total number of published and publicly available genomes are given. The number of publicly available genomes (*red line*) is higher than the number of published genomes (*blue line*), since in the case of genomes sequenced by the Joint Genome Institute those genomes are publicly available in MycoCosm well before being published (Reprinted with performance from Ref [219], Copyright © 2014 Elsevier)

4.8 Conclusion and Future Outlook

Depletion of fossil fuels in the world is one of the major reasons for increased biofuel research. Lignocellulose is one of the major alternative resource fulfill the current requirement for fuels and chemicals. The biofuel and paper pulp industries efficiently use cellulose in the production of paper and cellulosic ethanol, however lignin is left as a major industrial byproduct. Fungi are the most efficient lignin degrading microorganisms, producing several extra and intra cellular enzymes for breakdown of lignin. Understanding the lignin degrading mechanisms employed by white rot fungi is very important. Recent advances in the field of genomics and proteomics have revealed significant information about genes related to lignocellulose degradation and detoxification mechanisms. Whole genome sequences of *Phanerochaete chrysosporium, Postia placenta, Gloeophyllum trabeum* and *Dichomitus squalens* prove the occurrence of lignocellulolytic enzymes. Integrated computational analyses of proteome and secretome show that fungi undergo severe oxidative stress during the process of wood degradation, for which it employs various antioxidative and detoxification mechanisms. Application of advanced sequencing methodologies integrated with HPLC, GC and mass spectrometry techniques can help to elucidate the pathways involved in wood degradation.

References

1. Fengel D, Wegener G. Wood: chemistry, ultrastructure, reactions. Berlin: Walter de Gruyter; 1984. 613:1960–1982.
2. Whetten R, Sederoff R. Lignin biosynthesis. Plant Cell. 1995;7(7):1001.
3. Boerjan W, Ralph J, Baucher M. Lignin biosynthesis. Annu Rev Plant Biol. 2003;54(1):519–46.
4. Ten E, Ling C, Wang Y, Srivastava A, Dempere LA, Vermerris W. Lignin nanotubes as vehicles for gene delivery into human cells. Biomacromolecules. 2013;15(1):327–38.
5. Freudenberg K, Neish AC. Constitution and biosynthesis of lignin. Berlin/Heidelberg: Springer; 1968.
6. Higuchi T. Lignin biochemistry: biosynthesis and biodegradation. Wood Sci Technol. 1990;24(1):23–63.
7. Breznak JA, Brune A. Role of microorganisms in the digestion of lignocellulose by termites. Annu Rev Entomol. 1994;39(1):453–87.
8. Pandey MP, Kim CS. Lignin depolymerization and conversion: a review of thermochemical methods. Chem Eng Technol. 2011;34(1):29–41.
9. Wong DW. Structure and action mechanism of ligninolytic enzymes. Appl Biochem Biotechnol. 2009;157(2):174–209.
10. Hatakka A. Biodegradation of lignin. Biopolymers Online. 2005.
11. Arantes V, Goodell B. Current understanding of brown-rot fungal biodegradation mechanisms a review. In: Deterioration and protection of sustainable biomaterials, American chemical society symposium series. Washington, DC: American Chemical Society; 2014. p. 1–21.
12. Alexopoulos C, Mims C, Blackwell M. Introductory mycology. 4th ed. New York: Wiley; 1996, 869pp.
13. Leonowicz A, Matuszewska A, Luterek J, Ziegenhagen D, Wojtaś-Wasilewska M, Cho N-S, Hofrichter M, Rogalski J. Biodegradation of lignin by white rot fungi. Fungal Genet Biol. 1999;27(2):175–85.
14. Manavalan T, Manavalan A, Heese K. Characterization of lignocellulolytic enzymes from white-rot fungi. Curr Microbiol. 2015;70(4):485–98.
15. Kameshwar AKS, Qin W. Recent developments in using advanced sequencing technologies for the genomic studies of lignin and cellulose degrading microorganisms. Int J Biol Sci. 2016;12(2):156–71.
16. Cantarel BL, Coutinho PM, Rancurel C, Bernard T, Lombard V, Henrissat B. The Carbohydrate-Active EnZymes database (CAZy): an expert resource for glycogenomics. Nucleic Acids Res. 2009;37 suppl 1:D233–8.
17. Henrissat B. A classification of glycosyl hydrolases based on amino acid sequence similarities. Biochem J. 1991;280:309–16.
18. Levasseur A, Piumi F, Coutinho PM, Rancurel C, Asther M, Delattre M, Henrissat B, Pontarotti P, Asther M, Record E. FOLy: an integrated database for the classification and functional annotation of fungal oxidoreductases potentially involved in the degradation of lignin and related aromatic compounds. Fungal Genet Biol. 2008;45(5):638–45.
19. Blodig W, Smith AT, Doyle WA, Piontek K. Crystal structures of pristine and oxidatively processed lignin peroxidase expressed in Escherichia coli and of the W171F variant that eliminates the redox active tryptophan 171. Implications for the reaction mechanism. J Mol Biol. 2001;305(4):851–61.
20. Sundaramoorthy M, Youngs HL, Gold MH, Poulos TL. High-resolution crystal structure of manganese peroxidase: substrate and inhibitor complexes. Biochemistry. 2005;44(17):6463–70.
21. Hallberg BM, Henriksson G, Pettersson G, Divne C. Crystal structure of the flavoprotein domain of the extracellular flavocytochrome cellobiose dehydrogenase. J Mol Biol. 2002;315(3):421–34.

22. Dwivedi UN, Singh P, Pandey VP, Kumar A. Structure–function relationship among bacterial, fungal and plant laccases. J Mol Catal B Enzym. 2011;68(2):117–28.
23. Yoshida H. LXIII.-chemistry of lacquer (Urushi). Part I. Communication from the chemical society of Tokio. J Chem Soc Trans. 1883;43(0):472–86. doi:10.1039/CT8834300472.
24. Bertrand G. Sur la presence simultanee de la laccase et de la tyrosinase dans le suc de quelques champignons. CR Hebd Seances Acad Sci. 1896;123:463–5.
25. Heinzkill M, Messner K. The ligninolytic system of fungi. Fungal Biotechnol. 1997; 213–227.
26. Gianfreda L, Xu F, Bollag J-M. Laccases: a useful group of oxidoreductive enzymes. Bioremediation J. 1999;3(1):1–26.
27. O'Malley DM, Whetten R, Bao W, Chen CL, Sederoff RR. The role of laccase in lignification. Plant J. 1993;4(5):751–7.
28. Hatakka A. Lignin-modifying enzymes fungi: production and role. FEMS Microbiol Rev. 1994;13:125–35.
29. Youn H-D, Hah YC, Kang S-O. Role of laccase in lignin degradation by white-rot fungi. FEMS Microbiol Lett. 1995;132(3):183–8.
30. Thurston CF. The structure and function of fungal laccases. Microbiology. 1994;140(1):19–26.
31. Leatham GF, Stahmann MA. Studies on the laccase of Lentinus edodes: specificity, localization and association with the development of fruiting bodies. J Gen Microbiol. 1981;125(1):147–57.
32. Ikegaya N, Goto M, Hayashi Y. Effect of phenolic compounds and urovides on the activities of extracellular enzyme during vegetative growth and fruit-body formation of Lentinus edodes. Transactions of the Mycological Society of Japan (Japan). 1993.
33. Worrall J, Chet I, Hüttermann A. Association of rhizomorph formation with laccase activity in Armillaria spp. J Gen Microbiol. 1986;132(9):2527–33.
34. Viterbo A, Staples RC, Yagen B, Mayer AM. Selective mode of action of cucurbitacin in the inhibition of laccase formation in Botrytis cinerea. Phytochemistry. 1994;35(5):1137–42.
35. Piontek K, Antorini M, Choinowski T. Crystal structure of a laccase from the fungus Trametes versicolor at 1.90-Å resolution containing a full complement of coppers. J Biol Chem. 2002;277(40):37663–9.
36. Ducros V, Brzozowski AM, Wilson KS, Brown SH, Østergaard P, Schneider P, Yaver DS, Pedersen AH, Davies GJ. Crystal structure of the type-2 Cu depleted laccase from Coprinus cinereus at 2.2 Å resolution. Nat Struct Mol Biol. 1998;5(4):310–6.
37. Hakulinen N, Kiiskinen L-L, Kruus K, Saloheimo M, Paananen A, Koivula A, Rouvinen J. Crystal structure of a laccase from Melanocarpus albomyces with an intact trinuclear copper site. Nat Struct Mol Biol. 2002;9(8):601–5.
38. Lyashenko AV, Zhukhlistova NE, Gabdoulkhakov AG, Zhukova YN, Voelter W, Zaitsev VN, Bento I, Stepanova EV, Kachalova GS, Koroleva OV. Purification, crystallization and preliminary X-ray study of the fungal laccase from Cerrena maxima. Acta Crystallogr Sect F: Struct Biol Cryst Commun. 2006;62(10):954–7.
39. Kallio JP, Gasparetti C, Andberg M, Boer H, Koivula A, Kruus K, Rouvinen J, Hakulinen N. Crystal structure of an ascomycete fungal laccase from Thielavia arenaria–common structural features of asco-laccases. FEBS J. 2011;278(13):2283–95.
40. Ferraroni M, Myasoedova N, Schmatchenko V, Leontievsky A, Golovleva L, Scozzafava A, Briganti F. Crystal structure of a blue laccase from Lentinus tigrinus: evidences for intermediates in the molecular oxygen reductive splitting by multicopper oxidases. BMC Struct Biol. 2007;7(1):60.
41. Miki Y, Calviño FR, Pogni R, Giansanti S, Ruiz-Dueñas FJ, Martínez MJ, Basosi R, Romero A, Martínez AT. Crystallographic, kinetic, and spectroscopic study of the first ligninolytic peroxidase presenting a catalytic tyrosine. J Biol Chem. 2011;286(17):15525–34.
42. Edwards SL, Raag R, Wariishi H, Gold MH, Poulos TL. Crystal structure of lignin peroxidase. Proc Natl Acad Sci. 1993;90(2):750–4.

43. Piontek K, Smith A, Blodig W. Lignin peroxidase structure and function. Biochem Soc Trans. 2001;29(Pt 2):111–6.
44. Johjima T, Itoh N, Kabuto M, Tokimura F, Nakagawa T, Wariishi H, Tanaka H. Direct interaction of lignin and lignin peroxidase from Phanerochaete chrysosporium. Proc Natl Acad Sci. 1999;96(5):1989–94.
45. Blodig W, Smith AT, Winterhalter K, Piontek K. Evidence from spin-trapping for a transient radical on tryptophan residue 171 of lignin peroxidase. Arch Biochem Biophys. 1999;370(1):86–92.
46. Choinowski T, Blodig W, Winterhalter KH, Piontek K. The crystal structure of lignin peroxidase at 1.70 Å resolution reveals a hydroxy group on the C β of tryptophan 171: a novel radical site formed during the redox cycle. J Mol Biol. 1999;286(3):809–27.
47. Poulos T, Edwards S, Wariishi H, Gold M. Crystallographic refinement of lignin peroxidase at 2 A. J Biol Chem. 1993;268(6):4429–40.
48. Piontek K, Glumoff T, Winterhalter K. Low pH crystal structure of glycosylated lignin peroxidase from Phanerochaete chrysosporium at 2.5 Å resolution. FEBS Lett. 1993;315(2):119–24.
49. Sundaramoorthy M, Kishi K, Gold MH, Poulos TL. The crystal structure of manganese peroxidase from Phanerochaete chrysosporium at 2.06-A resolution. J Biol Chem. 1994;269(52):32759–67.
50. Sundaramoorthy M, Kishi K, Gold MH, Poulos TL. Crystal structures of substrate binding site mutants of manganese peroxidase. J Biol Chem. 1997;272(28):17574–80.
51. Sundaramoorthy M, Gold MH, Poulos TL. Ultrahigh (0.93 Å) resolution structure of manganese peroxidase from Phanerochaete chrysosporium: implications for the catalytic mechanism. J Inorg Biochem. 2010;104(6):683–90.
52. Pfister TD, Mirarefi AY, Gengenbach AJ, Zhao X, Danstrom C, Conatser N, Gao Y-G, Robinson H, Zukoski CF, Wang AH-J. Kinetic and crystallographic studies of a redesigned manganese-binding site in cytochrome c peroxidase. J Biol Inorg Chem. 2007;12(1):126–37.
53. Pogni R, Baratto MC, Teutloff C, Giansanti S, Ruiz-Dueñas FJ, Choinowski T, Piontek K, Martínez AT, Lendzian F, Basosi R. A Tryptophan Neutral Radical in the Oxidized State of Versatile Peroxidase from Pleurotus eryngii a combined multifrequency EPR and density functional theory study. J Biol Chem. 2006;281(14):9517–26.
54. Camarero S, Sarkar S, Ruiz-Dueñas FJ, Martınez MJ, Martınez ÁT. Description of a versatile peroxidase involved in the natural degradation of lignin that has both manganese peroxidase and lignin peroxidase substrate interaction sites. J Biol Chem. 1999;274(15):10324–30.
55. Ruiz-Dueñas FJ, Pogni R, Morales M, Giansanti S, Mate MJ, Romero A, Martínez MJ, Basosi R, Martínez AT. Protein radicals in fungal versatile peroxidase catalytic tryptophan radical in both compound I and compound II and studies on W164Y, W164H and W164S variants. J Biol Chem. 2009;284(12):7986–94.
56. Moreira PR, Duez C, Dehareng D, Antunes A, Almeida-Vara E, Frère J-M, Malcata FX, Duarte J. Molecular characterisation of a versatile peroxidase from a Bjerkandera strain. J Biotechnol. 2005;118(4):339–52.
57. Ruiz-Duenas FJ, Morales M, Mate MJ, Romero A, Martínez MJ, Smith AT, Martínez ÁT. Site-directed mutagenesis of the catalytic tryptophan environment in Pleurotus eryngii versatile peroxidase. Biochemistry. 2008;47(6):1685–95.
58. Henriksson G, Zhang L, Li J, Ljungquist P, Reitberger T, Pettersson G, Johansson G. Is cellobiose dehydrogenase from Phanerochaete chrysosporium a lignin degrading enzyme? Biochim Biophys Acta Protein Struct Mol Enzymol. 2000;1480(1):83–91.
59. Ferri S, Sode K. Amino acid substitution at the substrate-binding subsite alters the specificity of the Phanerochaete chrysosporium cellobiose dehydrogenase. Biochem Biophys Res Commun. 2010;391(2):1246–50.
60. Hallberg BM, Henriksson G, Pettersson G, Vasella A, Divne C. Mechanism of the reductive half-reaction in cellobiose dehydrogenase. J Biol Chem. 2003;278(9):7160–6.

61. Hallberg BM, Bergfors T, Bäckbro K, Pettersson G, Henriksson G, Divne C. A new scaffold for binding haem in the cytochrome domain of the extracellular flavocytochrome cellobiose dehydrogenase. Structure. 2000;8(1):79–88.
62. Albrecht Messerschmidt WS, Huber R, Lang G, Kroneck PM. X-ray crystallographic characterisation of type-2-depleted ascorbate oxidase from zucchini. Eur J Biochem. 1992;209:597–602.
63. Petersen LC, Degn H. Steady-state kinetics of laccase from Rhus vernicifera. Biochimica et Biophysica Acta (BBA)-Enzymology. 1978;526(1):85–92.
64. Giardina P, Faraco V, Pezzella C, Piscitelli A, Vanhulle S, Sannia G. Laccases: a never-ending story. Cell Mol Life Sci. 2010;67(3):369–85.
65. Solomon EI, Sundaram UM, Machonkin TE. Multicopper oxidases and oxygenases. Chem Rev. 1996;96(7):2563–606.
66. Yaropolov A, Skorobogat'Ko O, Vartanov S, Varfolomeyev S. Laccase. Appl Biochem Biotechnol. 1994;49(3):257–80.
67. Sakurai T. Anaerobic reactions of Rhus vernicifera laccase and its type-2 copper-depleted derivatives with hexacyanoferrate (II). Biochem J. 1992;284:681–5.
68. Höfer C, Schlosser D. Novel enzymatic oxidation of Mn 2+ to Mn 3+ catalyzed by a fungal laccase. FEBS Lett. 1999;451(2):186–90.
69. Schlosser D, Höfer C. Laccase-catalyzed oxidation of $Mn2^{+}$ in the presence of natural $Mn3^{+}$ chelators as a novel source of extracellular H_2O_2 production and its impact on manganese peroxidase. Appl Environ Microbiol. 2002;68(7):3514–21.
70. Bento I, Carrondo MA, Lindley PF. Reduction of dioxygen by enzymes containing copper. J Biol Inorg Chem. 2006;11(5):539–47.
71. Solomon EI, Baldwin MJ, Lowery MD. Electronic structures of active sites in copper proteins: contributions to reactivity. Chem Rev. 1992;92(4):521–42.
72. Palmieri G, Cennamo G, Faraco V, Amoresano A, Sannia G, Giardina P. Atypical laccase isoenzymes from copper supplemented Pleurotus ostreatus cultures. Enzym Microb Technol. 2003;33(2):220–30.
73. Leontievsky AA, Vares T, Lankinen P, Shergill JK, Pozdnyakova NN, Myasoedova NM, Kalkkinen N, Golovleva LA, Cammack R, Thurston CF. Blue and yellow laccases of ligninolytic fungi. FEMS Microbiol Lett. 1997;156(1):9–14.
74. Gutiérrez A, del Río JC, Ibarra D, Rencoret J, Romero J, Speranza M, Camarero S, Martínez MJ, Martínez ÁT. Enzymatic removal of free and conjugated sterols forming pitch deposits in environmentally sound bleaching of eucalypt paper pulp. Environ Sci Technol. 2006;40(10):3416–22.
75. Mikolasch A, Schauer F. Fungal laccases as tools for the synthesis of new hybrid molecules and biomaterials. Appl Microbiol Biotechnol. 2009;82(4):605–24.
76. Claus H. Laccases: structure, reactions, distribution. Micron. 2004;35(1):93–6.
77. Kawano T. Roles of the reactive oxygen species-generating peroxidase reactions in plant defense and growth induction. Plant Cell Rep. 2003;21(9):829–37.
78. Bansal N, Kanwar SS. Peroxidase (s) in environment protection. Sci World J. 2013;2013:1–9.
79. Perez-Boada M, Ruiz-Duenas FJ, Pogni R, Basosi R, Choinowski T, Martínez MJ, Piontek K, Martínez AT. Versatile peroxidase oxidation of high redox potential aromatic compounds: site-directed mutagenesis, spectroscopic and crystallographic investigation of three long-range electron transfer pathways. J Mol Biol. 2005;354(2):385–402.
80. Martınez AT. Molecular biology and structure-function of lignin-degrading heme peroxidases. Enzym Microb Technol. 2002;30(4):425–44.
81. Smith AT, Veitch NC. Substrate binding and catalysis in heme peroxidases. Curr Opin Chem Biol. 1998;2(2):269–78.
82. Banci L. Structural properties of peroxidases. J Biotechnol. 1997;53(2):253–63.
83. Gold M, Youngs H, Gelpke M. Manganese peroxidase. Met Ions Biol Syst. 2000;37:559.

84. Orth A, Denny M, Tien M. Overproduction of lignin-degrading enzymes by an isolate of Phanerochaete chrysosporium. Appl Environ Microbiol. 1991;57(9):2591–6.
85. Valli K, Wariishi H, Gold MH. Oxidation of monomethoxylated aromatic compounds by lignin peroxidase: role of veratryl alcohol in lignin biodegradation. Biochemistry. 1990;29(37):8535–9.
86. Johjima T, Wariishi H, Tanaka H. Veratryl alcohol binding sites of lignin peroxidase from Phanerochaete chrysosporium. J Mol Catal B Enzym. 2002;17(2):49–57.
87. Hammel KE, Cullen D. Role of fungal peroxidases in biological ligninolysis. Curr Opin Plant Biol. 2008;11(3):349–55.
88. Kersten PJ, Kalyanaraman B, Hammel KE, Reinhammar B, Kirk TK. Comparison of lignin peroxidase, horseradish peroxidase and laccase in the oxidation of methoxybenzenes. Biochem J. 1990;268:475–80.
89. Hammel KE, Kalyanaraman B, Kirk TK. Substrate free radicals are intermediates in ligninase catalysis. Proc Natl Acad Sci. 1986;83(11):3708–12.
90. Millis CD, Cai D, Stankovich MT, Tien M. Oxidation-reduction potentials and ionization states of extracellular peroxidases from the lignin-degrading fungus Phanerochaete chrysosporium. Biochemistry. 1989;28(21):8484–9.
91. Doyle WA, Blodig W, Veitch NC, Piontek K, Smith AT. Two substrate interaction sites in lignin peroxidase revealed by site-directed mutagenesis. Biochemistry. 1998;37(43):15097–105.
92. Mester T, Ambert-Balay K, Ciofi-Baffoni S, Banci L, Jones AD, Tien M. Oxidation of a tetrameric nonphenolic lignin model compound by lignin peroxidase. J Biol Chem. 2001;276(25):22985–90.
93. Baciocchi E, Fabbri C, Lanzalunga O. Lignin peroxidase-catalyzed oxidation of nonphenolic trimeric lignin model compounds: fragmentation reactions in the intermediate radical cations. J Org Chem. 2003;68(23):9061–9.
94. Bietti M, Baciocchi E, Steenken S. Lifetime, reduction potential and base-induced fragmentation of the veratryl alcohol radical cation in aqueous solution. Pulse radiolysis studies on a ligninase "mediator". J Phys Chem A. 1998;102(38):7337–42.
95. Candeias LP, Harvey PJ. Lifetime and reactivity of the veratryl alcohol radical cation. Implications for lignin peroxidase catalysis. J Biol Chem. 1995;270(28):16745–8.
96. Gilardi G, Harvey PJ, Cass AE, Palmer JM. Radical intermediates in veratryl alcohol oxidation by ligninase. NMR evidence. Biochim Biophys Acta Protein Struct Mol Enzymol. 1990;1041(2):129–32.
97. Cai D, Tien M. Kinetic studies on the formation and decomposition of compounds II and III. Reactions of lignin peroxidase with H_2O_2. J Biol Chem. 1992;267(16):11149–55.
98. Koduri RS, Tien M. Kinetic analysis of lignin peroxidase: explanation for the mediation phenomenon by veratryl alcohol. Biochemistry. 1994;33(14):4225–30.
99. Hofrichter M. Review: lignin conversion by manganese peroxidase (MnP). Enzym Microb Technol. 2002;30(4):454–66.
100. Glenn JK, Gold MH. Purification and characterization of an extracellular Mn (II)-dependent peroxidase from the lignin-degrading basidiomycete, Phanerochaete chrysosporium. Arch Biochem Biophys. 1985;242(2):329–41.
101. Paszczyński A, Huynh V-B, Crawford R. Enzymatic activities of an extracellular, manganese-dependent peroxidase from Phanerochaete chrysosporium. FEMS Microbiol Lett. 1985;29(1-2):37–41.
102. Tien M, Kirk TK. Lignin-degrading enzyme from the hymenomycete Phanerochaete chrysosporium Burds. Science (Washington). 1983;221(4611):661–2.
103. Glenn JK, Morgan MA, Mayfield MB, Kuwahara M, Gold MH. An extracellular H_2O_2-requiring enzyme preparation involved in lignin biodegradation by the white rot basidiomycete Phanerochaete chrysosporium. Biochem Biophys Res Commun. 1983;114(3):1077–83.
104. Pease EA, Tien M. Heterogeneity and regulation of manganese peroxidases from Phanerochaete chrysosporium. J Bacteriol. 1992;174(11):3532–40.

105. Glenn JK, Akileswaran L, Gold MH. Mn (II) oxidation is the principal function of the extracellular Mn-peroxidase from Phanerochaete chrysosporium. Arch Biochem Biophys. 1986;251(2):688–96.
106. Paszczyński A, Huynh V-B, Crawford R. Comparison of ligninase-I and peroxidase-M2 from the white-rot fungus Phanerochaete chrysosporium. Arch Biochem Biophys. 1986;244(2):750–65.
107. Wariishi H, Akileswaran L, Gold MH. Manganese peroxidase from the basidiomycete Phanerochaete chrysosporium: spectral characterization of the oxidized states and the catalytic cycle. Biochemistry. 1988;27(14):5365–70.
108. Wariishi H, Dunford HB, MacDonald I, Gold MH. Manganese peroxidase from the lignin-degrading basidiomycete Phanerochaete chrysosporium. Transient state kinetics and reaction mechanism. J Biol Chem. 1989;264(6):3335–40.
109. Wariishi H, Valli K, Gold MH. Manganese (II) oxidation by manganese peroxidase from the basidiomycete Phanerochaete chrysosporium. Kinetic mechanism and role of chelators. J Biol Chem. 1992;267(33):23688–95.
110. Wariishi H, Valli K, Gold MH. Oxidative cleavage of a phenolic diarylpropane lignin model dimer by manganese peroxidase from Phanerochaete chrysosporium. Biochemistry. 1989;28(14):6017–23.
111. Tuor U, Wariishi H, Schoemaker HE, Gold MH. Oxidation of phenolic arylglycerol. beta.-aryl ether lignin model compounds by manganese peroxidase from Phanerochaete chrysosporium: oxidative cleavage of an. alpha.-carbonyl model compound. Biochemistry. 1992;31(21):4986–95.
112. Reddy GVB, Sridhar M, Gold MH. Cleavage of nonphenolic β-1 diarylpropane lignin model dimers by manganese peroxidase from Phanerochaete chrysosporium. Eur J Biochem. 2003;270(2):284–92.
113. Wariishi H, Valli K, Renganathan V, Gold MH. Thiol-mediated oxidation of nonphenolic lignin model compounds by manganese peroxidase of Phanerochaete chrysosporium. J Biol Chem. 1989;264(24):14185–91.
114. Mester T, Tien M. Engineering of a manganese-binding site in lignin peroxidase isozyme H8 from Phanerochaete chrysosporium. Biochem Biophys Res Commun. 2001;284(3):723–8.
115. Timofeevski SL, Nie G, Reading NS, Aust SD. Addition of veratryl alcohol oxidase activity to manganese peroxidase by site-directed mutagenesis. Biochem Biophys Res Commun. 1999;256(3):500–4.
116. Ruiz-Dueñas FJ, Martínez MJ, Martínez AT. Molecular characterization of a novel peroxidase isolated from the ligninolytic fungus Pleurotus eryngii. Mol Microbiol. 1999;31(1):223–35.
117. Camarero S, Ruiz-Dueñas FJ, Sarkar S, Martínez MJ, Martínez AT. The cloning of a new peroxidase found in lignocellulose cultures of Pleurotus eryngii and sequence comparison with other fungal peroxidases. FEMS Microbiol Lett. 2000;191(1):37–43.
118. Ruiz-Dueñas FJ, Morales M, García E, Miki Y, Martínez MJ, Martínez AT. Substrate oxidation sites in versatile peroxidase and other basidiomycete peroxidases. J Exp Bot. 2009;60(2):441–52.
119. Henriksson G, Ander P, Pettersson B, Pettersson G. Cellobiose dehydrogenase (cellobiose oxidase) from Phanerochaete chrysosporium as a wood-degrading enzyme. Studies on cellulose, xylan and synthetic lignin. Appl Microbiol Biotechnol. 1995;42(5):790–6.
120. Kersten P, Cullen D. Extracellular oxidative systems of the lignin-degrading Basidiomycete Phanerochaete chrysosporium. Fungal Genet Biol. 2007;44(2):77–87.
121. Cameron MD, Aust SD. Cellobiose dehydrogenase–an extracellular fungal flavocytochrome. Enzym Microb Technol. 2001;28(2):129–38.
122. Henriksson G, Johansson G, Pettersson G. Is cellobiose oxidase from Phanerochaete chrysosporium a one-electron reductase? Biochim Biophys Acta Protein Struct Mol Enzymol. 1993;1144(2):184–90.

123. Morpeth FF. Some properties of cellobiose oxidase from the white-rot fungus Sporotrichum pulverulentum. Biochem J. 1985;228:557–64.
124. Henriksson G, Sild V, Szabó IJ, Pettersson G, Johansson G. Substrate specificity of cellobiose dehydrogenase from Phanerochaete chrysosporium. Biochim Biophys Acta Protein Struct Mol Enzymol. 1998;1383(1):48–54.
125. Henriksson G, Johansson G, Pettersson G. A critical review of cellobiose dehydrogenases. J Biotechnol. 2000;78(2):93–113.
126. Baldrian P, Valášková V. Degradation of cellulose by basidiomycetous fungi. FEMS Microbiol Rev. 2008;32(3):501–21.
127. Henriksson G, Pettersson G, Johansson G, Ruiz A, Uzcategui E. Cellobiose oxidase from Phanerochaete chrysosporium can be cleaved by papain into two domains. Eur J Biochem. 1991;196(1):101–6.
128. Ander P. The cellobiose-oxidizing enzymes CBQ and CbO as related to lignin and cellulose degradation– a review. FEMS Microbiol Rev. 1994;13(2):297–312.
129. Archibald F, Bourbonnais R, Jurasek L, Paice M, Reid I. Kraft pulp bleaching and delignification by Trametes versicolor. J Biotechnol. 1997;53(2):215–36.
130. Cameron MD, Aust SD. Degradation of chemicals by reactive radicals produced by cellobiose dehydrogenase from Phanerochaete chrysosporium. Arch Biochem Biophys. 1999;367(1):115–21.
131. Fernández IS, Ruiz-Duenas FJ, Santillana E, Ferreira P, Martínez MJ, Martínez ÁT, Romero A. Novel structural features in the GMC family of oxidoreductases revealed by the crystal structure of fungal aryl-alcohol oxidase. Acta Crystallogr D Biol Crystallogr. 2009;65(11):1196–205.
132. van den Heuvel RH, van den Berg WA, Rovida S, van Berkel WJ. Laboratory-evolved vanillyl-alcohol oxidase produces natural vanillin. J Biol Chem. 2004;279(32):33492–500.
133. Wohlfahrt G, Witt S, Hendle J, Schomburg D, Kalisz HM, Hecht H-J. 1.8 and 1.9 Å resolution structures of the Penicillium amagasakiense and Aspergillus niger glucose oxidases as a basis for modelling substrate complexes. Acta Crystallogr D Biol Crystallogr. 1999;55(5):969–77.
134. Rannes JB, Ioannou A, Willies SC, Grogan G, Behrens C, Flitsch SL, Turner NJ. Glycoprotein labeling using engineered variants of galactose oxidase obtained by directed evolution. J Am Chem Soc. 2011;133(22):8436–9.
135. Hassan N, Tan T-C, Spadiut O, Pisanelli I, Fusco L, Haltrich D, Peterbauer CK, Divne C. Crystal structures of Phanerochaete chrysosporium pyranose 2-oxidase suggest that the N-terminus acts as a propeptide that assists in homotetramer assembly. FEBS Open Bio. 2013;3:496–504.
136. Shah V, Nerud F. Lignin degrading system of white-rot fungi and its exploitation for dye decolorization. Can J Microbiol. 2002;48(10):857–70.
137. Ferreira P, Medina M, Guillén F, Martinez M, Van Berkel W, Martinez A. Spectral and catalytic properties of aryl-alcohol oxidase, a fungal flavoenzyme acting on polyunsaturated alcohols. Biochem J. 2005;389:731–8.
138. Farmer V, Henderson ME, Russell J. Aromatic-alcohol-oxidase activity in the growth medium of Polystictus versicolor. Biochem J. 1960;74(2):257.
139. Guillén F, Martinez AT, Martínez MJ. Production of hydrogen peroxide by aryl-alcohol oxidase from the ligninolytic fungus Pleurotus eryngii. Appl Microbiol Biotechnol. 1990;32(4):465–9.
140. Muheim A, Waldner R, Leisola MS, Fiechter A. An extracellular aryl-alcohol oxidase from the white-rot fungus Bjerkandera adusta. Enzym Microb Technol. 1990;12(3):204–9.
141. Kim SJ, Suzuki N, Uematsu Y, Shoda M. Characterization of aryl alcohol oxidase produced by dye-decolorizing fungus, geotrichum candidum decl. J Biosci Bioeng. 2001;91(2):166–72.

142. Guillen F, Martinez AT, Martinez MJ. Substrate specificity and properties of the aryl-alcohol oxidase from the ligninolytic fungus Pleurotus eryngii. Eur J Biochem. 1992;209(2):603–11.
143. Varela E, Martinez A, Martinez M. Molecular cloning of aryl-alcohol oxidase from the fungus Pleurotus eryngii, an enzyme involved in lignin degradation. Biochem J. 1999;341:113–7.
144. Hernández-Ortega A, Ferreira P, Martínez AT. Fungal aryl-alcohol oxidase: a peroxide-producing flavoenzyme involved in lignin degradation. Appl Microbiol Biotechnol. 2012;93(4):1395–410.
145. Varela E, Martınez MJ, Martınez AT. Aryl-alcohol oxidase protein sequence: a comparison with glucose oxidase and other FAD oxidoreductases. Biochim Biophys Acta Protein Struct Mol Enzymol. 2000;1481(1):202–8.
146. Hecht H, Kalisz H, Hendle J, Schmid R, Schomburg D. Crystal structure of glucose oxidase from Aspergillus niger refined at 2·3 Å reslution. J Mol Biol. 1993;229(1):153–72.
147. Pazur JH, Kleppe K. The oxidation of glucose and related compounds by glucose oxidase from Aspergillus niger*. Biochemistry. 1964;3(4):578–83.
148. Wierenga RK, Terpstra P, Hol WG. Prediction of the occurrence of the ADP-binding βαβ-fold in proteins, using an amino acid sequence fingerprint. J Mol Biol. 1986;187(1):101–7.
149. Gutierrez A, Caramelo L, Prieto A, Martínez MJ, Martinez AT. Anisaldehyde production and aryl-alcohol oxidase and dehydrogenase activities in ligninolytic fungi of the genus Pleurotus. Appl Environ Microbiol. 1994;60(6):1783–8.
150. Romero E, Ferreira P, Martínez ÁT, Martínez MJ. New oxidase from Bjerkandera arthroconidial anamorph that oxidizes both phenolic and nonphenolic benzyl alcohols. Biochim Biophys Acta Protein Struct Mol Enzymol. 2009;1794(4):689–97.
151. Hernández-Ortega A, Ferreira P, Merino P, Medina M, Guallar V, Martínez AT. Stereoselective hydride transfer by aryl-alcohol oxidase, a member of the GMC superfamily. ChemBioChem. 2012;13(3):427–35.
152. Ferreira P, Hernández-Ortega A, Lucas F, Carro J, Herguedas B, Borrelli KW, Guallar V, Martínez AT, Medina M. Aromatic stacking interactions govern catalysis in aryl-alcohol oxidase. FEBS J. 2015;282:3091–106.
153. van den Heuvel RH, Fraaije MW, Mattevi A, van Berkel WJ. Asp-170 is crucial for the redox properties of vanillyl-alcohol oxidase. J Biol Chem. 2000;275(20):14799–808.
154. van den Heuvel RH, Fraaije MW, Mattevi A, Laane C, van Berkel WJ. Vanillyl-alcohol oxidase, a tasteful biocatalyst. J Mol Catal B Enzym. 2001;11(4):185–8.
155. Fraaije MW, van Berkel WJ. Catalytic mechanism of the oxidative demethylation of 4-(Methoxymethyl) phenol by vanillyl-alcohol oxidase evidence for formation of a p-quinone methide intermediate. J Biol Chem. 1997;272(29):18111–6.
156. Mattevi A, Fraaije MW, Mozzarelli A, Olivi L, Coda A, van Berkel WJ. Crystal structures and inhibitor binding in the octameric flavoenzyme vanillyl-alcohol oxidase: the shape of the active-site cavity controls substrate specificity. Structure. 1997;5(7):907–20.
157. van den Heuvel RH, Fraaije MW, Mattevi A, van Berkel WJ Structure, function and redesign of vanillyl-alcohol oxidase. In: International Congress Series, 2002. Elsevier, p. 13–24
158. van den Heuvel RH, Fraaije MW, Ferrer M, Mattevi A, van Berkel WJ. Inversion of stereospecificity of vanillyl-alcohol oxidase. Proc Natl Acad Sci. 2000;97(17):9455–60.
159. Whittaker MM, Kersten PJ, Nakamura N, Sanders-Loehr J, Schweizer ES, Whittaker JW. Glyoxal oxidase from Phanerochaete chrysosporium is a new radical-copper oxidase. J Biol Chem. 1996;271(2):681–7.
160. Whittaker MM, Kersten PJ, Cullen D, Whittaker JW. Identification of catalytic residues in glyoxal oxidase by targeted mutagenesis. J Biol Chem. 1999;274(51):36226–32.
161. Kersten PJ, Kirk TK. Involvement of a new enzyme, glyoxal oxidase, in extracellular H_2O_2 production by Phanerochaete chrysosporium. J Bacteriol. 1987;169(5):2195–201.

162. Kersten PJ, Cullen D. Cloning and characterization of cDNA encoding glyoxal oxidase, a H_2O_2-producing enzyme from the lignin-degrading basidiomycete Phanerochaete chrysosporium. Proc Natl Acad Sci. 1993;90(15):7411–3.
163. Itoh S, Hirano K, Furuta A, Komatsu M, Ohshiro Y, Ishida A, Takamuku S, Kohzuma T, Nakamura N, Suzuki S. Physicochemical properties of 2-Methylthio-4-methylphenol, a model compound of the novel cofactor of galactose oxidase. Chem Lett. 1993;12:2099–102.
164. Kersten PJ, Witek C, Vanden Wymelenberg A, Cullen D. Phanerochaete chrysosporium glyoxal oxidase is encoded by two allelic variants: structure, genomic organization, and heterologous expression of glx1 and glx2. J Bacteriol. 1995;177(21):6106–10.
165. Danneel HJ, Rossner E, Zeeck A, Giffhorn F. Purification and characterization of a pyranose oxidase from the basidiomycete Peniophora gigantea and chemical analyses of its reaction products. Eur J Biochem. 1993;214(3):795–802.
166. Izumi Y, Furuya Y, Yamada H. Purification and properties of pyranose oxidase from basidiomycetous fungus no. 52. Agric Biol Chem. 1990;54(6):1393–9.
167. Machida Y, Nakanishi T. Purification and properties of pyranose oxidase from Coriolus versicolor. Agric Biol Chem. 1984;48(10):2463–70.
168. Daniel G, Volc J, Kubatova E. Pyranose oxidase, a major source of H_2O_2 during wood degradation by Phanerochaete chrysosporium, Trametes versicolor, and Oudemansiella mucida. Appl Environ Microbiol. 1994;60(7):2524–32.
169. Cavener DR. GMC oxidoreductases: a newly defined family of homologous proteins with diverse catalytic activities. J Mol Biol. 1992;223(3):811–4.
170. Hallberg BM, Leitner C, Haltrich D, Divne C. Crystal structure of the 270 kDa homotetrameric lignin-degrading enzyme pyranose 2-oxidase. J Mol Biol. 2004;341(3):781–96.
171. Giffhorn F. Fungal pyranose oxidases: occurrence, properties and biotechnical applications in carbohydrate chemistry. Appl Microbiol Biotechnol. 2000;54(6):727–40.
172. Volc J, Sedmera P, Havlíček V, Přikrylová V, Daniel G. Conversion of D-glucose to D-erythro-hexos-2, 3-diulose (2, 3-diketo-D-glucose) by enzyme preparations from the basidiomycete Oudemansiella mucida. Carbohydr Res. 1995;278(1):59–70.
173. Freimund S, Huwig A, Giffhorn F, Köpper S. Rare keto-aldoses from enzymatic oxidation: substrates and oxidation products of pyranose 2-oxidase. Chem Eur J. 1998;4(12):2442–55.
174. Giffhorn F, Köpper S, Huwig A, Freimund S. Rare sugars and sugar-based synthons by chemo-enzymatic synthesis. Enzym Microb Technol. 2000;27(10):734–42.
175. Baron AJ, Stevens C, Wilmot C, Seneviratne KD, Blakeley V, Dooley DM, Phillips S, Knowles PF, McPherson MJ. Structure and mechanism of galactose oxidase. The free radical site. J Biol Chem. 1994;269(40):25095–105.
176. Firbank S, Rogers M, Wilmot C, Dooley D, Halcrow M, Knowles P, McPherson M, Phillips S. Crystal structure of the precursor of galactose oxidase: an unusual self-processing enzyme. Proc Natl Acad Sci. 2001;98(23):12932–7.
177. Yin D, Urresti S, Lafond M, Johnston EM, Derikvand F, Ciano L, Berrin J-G, Henrissat B, Walton PH, Davies GJ, Brumer H. Structure-function characterization reveals new catalytic diversity in the galactose oxidase and glyoxal oxidase family. Nat Commun. 2015;6:10197. doi:10.1038/ncomms10197.
178. Ito N, Phillips SE, Stevens C, Ogel ZB, McPherson MJ, Keen JN, Yadav KD, Knowles PF. Novel thioether bond revealed by a 1.7 Å crystal structure of galactose oxidase. Nature. 1991;350:87–90.
179. Bankar SB, Bule MV, Singhal RS, Ananthanarayan L. Glucose oxidase—an overview. Biotechnol Adv. 2009;27(4):489–501.
180. Hatzinikolaou D, Macris B. Factors regulating production of glucose oxidase by Aspergillus niger. Enzym Microb Technol. 1995;17(6):530–4.
181. Kapat A, Jung J, Park Y. Enhancement of glucose oxidase production in batch cultivation of recombinant Saccharomyces cerevisiae: optimization of oxygen transfer condition. J Appl Microbiol. 2001;90(2):216–22.

182. Kalisz H, Hendle J, Schmid R. Structural and biochemical properties of glycosylated and deglycosylated glucose oxidase from Penicillium amagasakiense. Appl Microbiol Biotechnol. 1997;47(5):502–7.
183. Kusai K, Sekuzu I, Hagihara B, Okunuki K, Yamauchi S, Nakai M. Crystallization of glucose oxidase from Penicillium amagasakiense. Biochim Biophys Acta. 1960;40:555–7.
184. Nakamura S, FUJIKI S. Comparative studies on the glucose oxidases of Aspergillus niger and Penicillium amagasakiense. J Biochem. 1968;63(1):51–8.
185. Witt S, Wohlfahrt G, Schomburg D, Hecht H, Kalisz H. Conserved arginine-516 of Penicillium amagasakiense glucose oxidase is essential for the efficient binding of β-D-glucose. Biochem J. 2000;347:553–9.
186. Witteveen CF, Veenhuis M, Visser J. Localization of glucose oxidase and catalase activities in Aspergillus niger. Appl Environ Microbiol. 1992;58(4):1190–4.
187. Raba J, Mottola HA. Glucose oxidase as an analytical reagent. Crit Rev Anal Chem. 1995;25(1):1–42.
188. Brock BJ, Rieble S, Gold MH. Purification and Characterization of a 1, 4-Benzoquinone Reductase from the Basidiomycete Phanerochaete chrysosporium. Appl Environ Microbiol. 1995;61(8):3076–81.
189. Akileswaran L, Brock BJ, Cereghino JL, Gold MH. 1, 4-Benzoquinone reductase from Phanerochaete chrysosporium: cDNA cloning and regulation of expression. Appl Environ Microbiol. 1999;65(2):415–21.
190. Brock BJ, Gold MH. 1, 4-Benzoquinone reductase from the basidiomycetePhanerochaete chrysosporium: spectral and kinetic analysis. Arch Biochem Biophys. 1996;331(1):31–40.
191. Aitor H-O, Kenneth B, Patricia F, Milagros M, Angel TM, Victor G. Substrate diffusion and oxidation in GMC oxidoreductases: an experimental and computational study on fungal aryl-alcohol oxidase. Biochem J. 2011;436(2):341–50.
192. Hernández-Ortega A, Lucas F, Ferreira P, Medina M, Guallar V, Martínez AT. Modulating O_2 reactivity in a fungal flavoenzyme involvement of aryl-alcohol oxidase PHE-501 contiguous to catalytic histidine. J Biol Chem. 2011;286(47):41105–14.
193. Hernández-Ortega A, Lucas F, Ferreira P, Medina M, Guallar V, Martínez AT. Role of active site histidines in the two half-reactions of the aryl-alcohol oxidase catalytic cycle. Biochemistry. 2012;51(33):6595–608.
194. Fraaije MW, van den Heuvel RH, van Berkel WJ, Mattevi A. Covalent flavinylation is essential for efficient redox catalysis in vanillyl-alcohol oxidase. J Biol Chem. 1999;274(50):35514–20.
195. Fraaije MW, van den Heuvel RH, van Berkel WJ, Mattevi A. Structural analysis of flavinylation in vanillyl-alcohol oxidase. J Biol Chem. 2000;275(49):38654–8.
196. Vaidyanathan M, Palaniandavar M, Gopalan RS. Copper (II) complexes of sterically hindered phenolate ligands as structural models for the active site in galactose oxidase and glyoxal oxidase: x-ray crystal structure and spectral and redox properties. Inorg Chim Acta. 2001;324(1):241–51.
197. Halfen JA, Jazdzewski BA, Mahapatra S, Berreau LM, Wilkinson EC, Que L, Tolman WB. Synthetic models of the inactive copper (II)-tyrosinate and active copper (II)-tyrosyl radical forms of galactose and glyoxal oxidases. J Am Chem Soc. 1997;119(35):8217–27.
198. Kujawa M, Ebner H, Leitner C, Hallberg BM, Prongjit M, Sucharitakul J, Ludwig R, Rudsander U, Peterbauer C, Chaiyen P. Structural basis for substrate binding and regioselective oxidation of monosaccharides at C3 by pyranose 2-oxidase. J Biol Chem. 2006;281(46):35104–15.
199. Pitsawong W, Sucharitakul J, Prongjit M, Tan T-C, Spadiut O, Haltrich D, Divne C, Chaiyen P. A conserved active-site threonine is important for both sugar and flavin oxidations of pyranose 2-oxidase. J Biol Chem. 2010;285(13):9697–705.
200. Spadiut O, Tan TC, Pisanelli I, Haltrich D, Divne C. Importance of the gating segment in the substrate-recognition loop of pyranose 2-oxidase. FEBS J. 2010;277(13):2892–909.

201. Heckmann-Pohl DM, Bastian S, Altmeier S, Antes I. Improvement of the fungal enzyme pyranose 2-oxidase using protein engineering. J Biotechnol. 2006;124(1):26–40.
202. Bannwarth M, Heckmann-Pohl D, Bastian S, Giffhorn F, Schulz GE. Reaction geometry and thermostable variant of pyranose 2-oxidase from the white-rot fungus Peniophora sp. Biochemistry. 2006;45(21):6587–95.
203. Rogers MS, Tyler EM, Akyumani N, Kurtis CR, Spooner RK, Deacon SE, Tamber S, Firbank SJ, Mahmoud K, Knowles PF. The stacking tryptophan of galactose oxidase: a second-coordination sphere residue that has profound effects on tyrosyl radical behavior and enzyme catalysis. Biochemistry. 2007;46(15):4606–18.
204. Ito N, Phillips SE, Yadav KD, Knowles PF. Crystal structure of a free radical enzyme, galactose oxidase. J Mol Biol. 1994;238(5):704–814.
205. Hecht H, Schomburg D, Kalisz H, Schmid R. The 3D structure of glucose oxidase from Aspergillus niger. Implications for the use of GOD as a biosensor enzyme. Biosens Bioelectron. 1993;8(3):197–203.
206. Martinez D, Larrondo LF, Putnam N, Gelpke MDS, Huang K, Chapman J, Helfenbein KG, Ramaiya P, Detter JC, Larimer F. Genome sequence of the lignocellulose degrading fungus Phanerochaete chrysosporium strain RP78. Nat Biotechnol. 2004;22(6):695–700.
207. Wymelenberg AV, Minges P, Sabat G, Martinez D, Aerts A, Salamov A, Grigoriev I, Shapiro H, Putnam N, Belinky P. Computational analysis of the Phanerochaete chrysosporium v2. 0 genome database and mass spectrometry identification of peptides in ligninolytic cultures reveal complex mixtures of secreted proteins. Fungal Genet Biol. 2006;43(5):343–56.
208. Martinez D, Challacombe J, Morgenstern I, Hibbett D, Schmoll M, Kubicek CP, Ferreira P, Ruiz-Duenas FJ, Martinez AT, Kersten P. Genome, transcriptome, and secretome analysis of wood decay fungus Postia placenta supports unique mechanisms of lignocellulose conversion. Proc Natl Acad Sci. 2009;106(6):1954–9.
209. Eastwood DC, Floudas D, Binder M, Majcherczyk A, Schneider P, Aerts A, Asiegbu FO, Baker SE, Barry K, Bendiksby M. The plant cell wall–decomposing machinery underlies the functional diversity of forest fungi. Science. 2011;333(6043):762–5.
210. Tang JD, Perkins AD, Sonstegard TS, Schroeder SG, Burgess SC, Diehl SV. Short-read sequencing for genomic analysis of the brown rot fungus Fibroporia radiculosa. Appl Environ Microbiol. 2012;78(7):2272–81.
211. Ohm RA, De Jong JF, Lugones LG, Aerts A, Kothe E, Stajich JE, De Vries RP, Record E, Levasseur A, Baker SE. Genome sequence of the model mushroom Schizophyllum commune. Nat Biotechnol. 2010;28(9):957–63.
212. Fernandez-Fueyo E, Ruiz-Dueñas FJ, Ferreira P, Floudas D, Hibbett DS, Canessa P, Larrondo LF, James TY, Seelenfreund D, Lobos S. Comparative genomics of Ceriporiopsis subvermispora and Phanerochaete chrysosporium provide insight into selective ligninolysis. Proc Natl Acad Sci. 2012;109(14):5458–63.
213. Suzuki H, MacDonald J, Syed K, Salamov A, Hori C, Aerts A, Henrissat B, Wiebenga A, Barry K, Lindquist E. Comparative genomics of the white-rot fungi, Phanerochaete carnosa and P. chrysosporium, to elucidate the genetic basis of the distinct wood types they colonize. BMC Genomics. 2012;13(1):444.
214. Olson Å, Aerts A, Asiegbu F, Belbahri L, Bouzid O, Broberg A, Canbäck B, Coutinho PM, Cullen D, Dalman K. Insight into trade-off between wood decay and parasitism from the genome of a fungal forest pathogen. New Phytol. 2012;194(4):1001–13.
215. Martin F, Aerts A, Ahrén D, Brun A, Danchin E, Duchaussoy F, Gibon J, Kohler A, Lindquist E, Pereda V. The genome of Laccaria bicolor provides insights into mycorrhizal symbiosis. Nature. 2008;452(7183):88–92.
216. Bao D, Gong M, Zheng H, Chen M, Zhang L, Wang H, Jiang J, Wu L, Zhu Y, Zhu G. Sequencing and comparative analysis of the straw mushroom (Volvariella volvacea) genome. PLoS One. 2013;8(3), e58294.
217. Morin E, Kohler A, Baker AR, Foulongne-Oriol M, Lombard V, Nagye LG, Ohm RA, Patyshakuliyeva A, Brun A, Aerts AL. Genome sequence of the button mushroom Agaricus

bisporus reveals mechanisms governing adaptation to a humic-rich ecological niche. Proc Natl Acad Sci. 2012;109(43):17501–6.
218. Collins C, Keane TM, Turner DJ, O'Keeffe G, Fitzpatrick DA, Doyle S. Genomic and proteomic dissection of the ubiquitous plant pathogen, Armillaria mellea: toward a new infection model system. J Proteome Res. 2013;12(6):2552–70.
219. Ohm RA, Riley R, Salamov A, Min B, Choi I-G, Grigoriev IV. Genomics of wood-degrading fungi. Fungal Genet Biol. 2014;72:82–90.
220. Floudas D, Binder M, Riley R, Barry K, Blanchette RA, Henrissat B, Martínez AT, Otillar R, Spatafora JW, Yadav JS. The Paleozoic origin of enzymatic lignin decomposition reconstructed from 31 fungal genomes. Science. 2012;336(6089):1715–9.
221. Hofrichter M, Ullrich R, Pecyna MJ, Liers C, Lundell T. New and classic families of secreted fungal heme peroxidases. Appl Microbiol Biotechnol. 2010;87(3):871–97.
222. Grigoriev IV, Nikitin R, Haridas S, Kuo A, Ohm R, Otillar R, Riley R, Salamov A, Zhao X, Korzeniewski F. MycoCosm portal: gearing up for 1000 fungal genomes. Nucleic Acids Res. 2013;42:D699–704.